

Amortising Variational Bayesian Inference over prior hyperparameters with a Normalising Flow

Laura Battaglia* and Geoff Nicholls†

Abstract. In Bayesian inference prior hyperparameters are chosen subjectively or estimated using empirical Bayes methods. Generalised Bayesian Inference also has hyperparameters (the learning rate, and parameters of the loss). As part of the Generalised-Bayes workflow it is necessary to check sensitivity to the choice of hyperparameters, but running MCMC or fitting a variational approximation at each hyperparameter setting is impractical when there are more than a few hyperparameters. Simulation Based Inference has been used to amortise over data and hyperparameters and can be useful for Bayesian problems. However, there is no Simulation Based Inference for Generalised Bayes posteriors, as there is no generative model for the data. Working with a variational family parameterised by a normalising flow, we show how to fit a variational Generalised Bayes posterior, amortised over all hyperparameters. This may be sampled very efficiently at different hyperparameter values without refitting, and supports efficient robustness checks and hyperparameter selection. We show that there exist amortised normalising-flow architectures which are universal approximators. We test our approach on a relatively large-scale application of Generalised Bayesian Inference. The code is available online.

Keywords: Generalised Bayes, Variational Inference, Normalising Flow, Hyperparameters.

1 Introduction

Posterior probability distributions are commonly indexed by hyperparameters. These include prior hyperparameters and the kind of learning-rate parameters that enter Generalised Bayesian Inference (GBI, Bissiri et al. (2016); Grünwald and Ommen (2017)). In many workflows it is necessary to check how posterior expectations depend on hyperparameter values, a time consuming task requiring multiple MCMC runs or variational approximations. Developing ideas from Carmona and Nicholls (2022), we show that the analysis may be done using a single variational approximation to the whole family of posteriors. We fit this in a single end-to-end optimisation pass. The fitted approximation, called the Variational Meta-Posterior (VMP), makes it is easy to check robustness and select hyperparameters.

A variational approximation to a posterior is “amortised over the data” if the fitted variational density takes the data as in input and approximates the posterior at any realisation of the data. This generally uses training data simulated from the observation model. We will amortise over hyperparameters, and avoid amortising over data, in

*Department of Statistics, University of Oxford, UK, laura.battaglia@stats.ox.ac.uk

†Department of Statistics, University of Oxford, UK, nicholls@stats.ox.ac.uk

order to get a method which works for GBI, where no normalised probability distribution representing the observation model exists. A good variational approximation to the true family of posteriors is needed so we use a normalising flow (Rezende and Mohamed (2015); for a review, see Papamakarios et al. (2021)). A general normalising flow is a diffeomorphism mapping unstructured random variables with simple probability densities to structured random variables distributed according to the target distribution, which in our case is the posterior. Flow-parameters are in general chosen to approximate a single target posterior. However, the VMP is amortised over hyperparameters at training. It takes prior hyperparameters as additional inputs to its flow-conditioner functions and this allows a single set of flow-parameters to determine the variational approximation at any set of hyperparameter values.

It is known (Huang et al., 2018; Papamakarios et al., 2021) that a masked autoregressive flow is a universal approximator for a single target posterior (under regularity conditions). We replace the additive conditioner in Carmona and Nicholls (2022) with a more general non-linear conditioner and show that this VMP simultaneously and universally approximates any target family of posterior densities (under the same regularity conditions applied to each density in the family). No real flow is a universal approximator. Also, masked autoregressive flows are expensive to invert, so we implement a neural spline flow (Durkan et al., 2019) and compose maps with simpler coupling-layer conditioners (Dinh et al., 2016), conceding expressive power for efficiency gains.

We can use the fitted VMP to efficiently explore the dependence of posterior expectations on hyperparameter settings. In some settings we may go further and estimate them. Values maximising the marginal likelihood are commonly taken. We use this in a simple example with synthetic data in Section 6.1. This kind of Empirical Bayes approach (Robbins, 1956) is common in the ML literature (and may be found in the original papers on Variational Auto-Encoders (Kingma and Welling, 2013) and flows (Rezende and Mohamed, 2015) where they maximise the ELBO). However, the marginal likelihood is known to be inappropriate when the model is misspecified (Grünwald and Ommen, 2017; Gelman and Yao, 2020; Fortuin, 2022). In Carmona and Nicholls (2022) and Frazier and Nott (2023a), the importance of using a loss that reflects the goals of the inference is highlighted. We illustrate our methods with a loss for prediction (the Expected Log Pointwise Prediction Density or ELPD) in Section 6.2 and another for parameter estimation (the Posterior Mean Squared Error or PMSE) in Section 6.3.

2 Related work and contribution

2.1 Related work

The literature on data-amortisation in contexts like Amortised VI (A-VI, Gershman and Goodman (2014), Margossian and Blei (2023)) and Forward Amortised VI (FAVI, Ambrogioni et al. (2019)) parallels our work. A-VI learns a single deterministic map predicting variational factors for latent variables as a common function of the data associated with that point. This allows it to maximise a single Evidence Lower Bound objective in expectation over the data and obtain a single set of variational parameters

that work for all latent factors. In contrast FAVI optimises the forward KL by amortising over data. The resulting variational approximation is an explicit function of the data. We apply a similar procedure, but work with the reverse KL (precisely to avoid amortising over data), and amortise over hyperparameters.

Hyperparameter estimation is well-studied in the literature on VI and VAEs. Kingma and Welling (2013) makes a variational approximation to the posterior with a prior on hyperparameters. Wu et al. (2020) first amortise a VAE over data, maximising a lower bound on the marginal likelihood to estimate hyperparameters. However, they add a second layer of amortisation over data *distributions*, representing a data distribution by additional data samples. This improves generalisation. Finally, also related but in the specific context of Gaussian Processes, Liu et al. (2020) amortise over datasets to learn a unique mapping from data to kernel hyperparameters. Bitzer et al. (2023) generalises the approach to encompass different kernel structures.

Outside this literature but similar in purpose to our work is Giordano et al. (2022), who explore the sensitivity to hyperparameter choices in the context of Dirichlet process mixture models estimated with VI. Based on previous work on variational distribution expansions (Giordano et al., 2018), they build a linear approximation of the dependence of the variational optimum on the choice of the stick-breaking prior and its hyperparameters, and provide a computational tool to efficiently explore the sensitivity of the posterior quantities of interest to such a choice.

Specialised loss functions for the learning rate parameter in GBI are reviewed in Wu and Martin (2023). SafeBayes (Grünwald and Ommen, 2017), which achieves convergence over data at optimal rate to the pseudo-true, has strong support from theory. However, SafeBayes uses a sequential-predictive loss, so it needs n different posterior distributions for n data points, which is very computationally demanding. Holmes and Walker (2017) and Lyddon et al. (2019) use a criterion based on matching the expected information gain between Bayes and generalised Bayes updates. Syring and Martin (2019) and Winter et al. (2023) tune the learning rate so that posterior credible sets approximately achieve nominal frequentist coverage. Carmona and Nicholls (2020) target the WAIC (Watanabe, 2010; Vehtari et al., 2017). In general the appropriate loss will depend on the goals of the inference, and is decided on a case by case basis.

2.2 Our Contribution

Our work develops Carmona and Nicholls (2022) who give an amortised normalising flow parameterisation which defines a VMP. They estimate learning rate parameter vectors for GBI in settings where different factors in the likelihood have different learning rates. The dimension of the learning rate is high enough to rule out many of the methods for learning-rate estimation listed at the end of Section 2.1. Our analysis extends the earlier analysis by treating prior hyperparameters on the same footing as the learning rate. We also modify the VMP parameterisation given in Carmona and Nicholls (2022) and prove that the modified VMP is a universal approximator. As far as we know, this is the first result of this kind for any amortised variational scheme. Carmona et al. (2024) use the VMP to estimate a learning rate for the data we analyse in Section 6.3. We estimate both the learning rate and prior hyperparameters.

In recent independent work, [Elsemüller et al. \(2024\)](#) uses a variational framework, amortised over data, model and hyperparameters. The focus there is like our own: posterior sensitivity analysis. The setting is in fact more general, as sensitivity to variation in the model and data is also possible. They are interested in simulation-based inference, where the observation model is defined by a complex simulator and it is necessary to minimise the forward KL and amortise over data. The focus in [Elsemüller et al. \(2024\)](#) is on model comparison and hyperparameter estimation using the marginal likelihood, though they note in the supplement that other losses might be considered. This reflects their strictly Bayesian setting. We consider misspecified settings and GBI. In our setting data-amortisation is not possible, as there is no normalised generative model for the data, explicit or implicit. [Gao et al. \(2023\)](#) amortises an approximation to the loss itself, not the posterior. Finally, we give full detail of our flow parameterisation, as we need this for our new results on amortised universal approximation.

3 The Variational Meta-Posterior for approximate Bayesian inference

In Variational Inference ([Jordan et al. \(1999\)](#), [Wainwright et al. \(2008\)](#), [Blei et al. \(2017\)](#)) we define a family of “simple” densities $q(\theta; \lambda)$ with parameters $\lambda \in \Lambda$ and select the density which best approximates a target posterior density $p(\theta|Y, \psi)$ on p -dimensional parameters $\theta \in \Theta$ given data $Y \in \mathcal{Y}$ and fixed d_ψ -dimensional hyperparameters $\psi \in \Psi$. The universal approximator results in this paper require Θ and Ψ to be bounded sets and we assume $\Theta = \Theta_1 \times \Theta_2 \times \dots \times \Theta_p$ with $\theta_i \in \Theta_i$, $i = 1, \dots, p$ and similarly for Ψ .

If we wish to study the posterior at different hyperparameter-values then we can fit a separate variational approximation $q(\theta; \lambda)$, $\lambda \in \Lambda$ at each ψ of interest. At any given ψ we have flow parameters λ_ψ^* maximising the evidence lower bound (ELBO)

$$\lambda_\psi^* = \arg \max_{\lambda} \text{ELBO}(\lambda|\psi),$$

at fixed ψ , where

$$\text{ELBO}(\lambda|\psi) = E_{\theta \sim q(\theta; \lambda)} \left[\log \frac{p(\theta, Y|\psi)}{q(\theta; \lambda)} \right]. \quad (1)$$

If the variational family is sufficiently expressive then $p(\theta|Y, \psi) \simeq q(\theta; \lambda_\psi^*)$. We have to estimate λ_ψ^* separately at each ψ , so we have $\hat{\lambda}_\psi^*$ as a point estimate at each ψ -value in some small set of ψ -values of interest.

In fact there may exist a variational family $q(\theta; \lambda, \psi)$, $\lambda \in \Lambda$, and λ^* not depending on ψ , ensuring the approximation $p(\theta|Y, \psi) \simeq q(\theta; \lambda^*, \psi)$ holds uniformly over a range of ψ -values. This point is made, for the setting where ψ is a learning rate in GBI, in [Carmona and Nicholls \(2022\)](#) and applied to Bayesian hyperparameter estimation in [Elsemüller et al. \(2024\)](#). Following [Carmona and Nicholls \(2022\)](#), we call $q(\theta; \lambda, \psi)$, $\psi \in \Psi$ the *Variational Meta Posterior* (VMP).

3.1 Conditioned autoregressive flow

We now parameterise the amortised $q(\theta; \lambda, \psi)$. See Section A in the supplement for references and background on normalising flows. We adapt a neural autoregressive normalising flow based on user-supplied transformer and conditioner functions (Huang et al. (2018), Jaini et al. (2019)). This will define a transformation $T(\cdot; \lambda, \psi) : \mathbb{R}^p \rightarrow \mathbb{R}^p$ which is invertible and continuously differentiable in \mathbb{R}^p . For $q(\epsilon)$, $\epsilon \in \mathbb{R}^p$ some fixed simple distribution, for example, $U[0, 1]^p$ or $N(0_p, I_p)$, and $\epsilon \sim q(\cdot)$, the variational density $q(\theta; \lambda, \psi)$ is defined to be the density of $T(\epsilon; \lambda, \psi)$.

For $\epsilon \in \mathbb{R}^p$ let $\epsilon_{<i} = (\epsilon_1, \dots, \epsilon_{i-1})$. A transformer $\tau(\epsilon_i; h_i) \in R$ is a strictly monotone function of $\epsilon_i \in R$ with fixed parameters $h_i \in \mathbb{R}^{d_h}$ (for example, Durkan et al. (2019) takes τ to be a spline). A conditioner $c_i : \mathbb{R}^{-d_\psi + i - 1} \rightarrow \mathbb{R}^{d_h}$ is a map which returns a set of set of parameters for the transformer via $h_i = c_i(\epsilon_{<i}, \psi; \lambda_i)$, in our case a Multi-Layer Perceptron (MLP). The transformation $(\theta_1, \dots, \theta_p) = T(\epsilon; \lambda, \psi)$ is

$$\begin{aligned} \theta_1 &= \tau(\epsilon_1, h_1), & h_1 &= c_1(\psi; \lambda_1), \\ \theta_i &= \tau(\epsilon_i, h_i), & h_i &= c_i(\epsilon_{<i}, \psi; \lambda_i), \quad i = 2, \dots, p. \end{aligned} \quad (2)$$

The only change to the usual setup (Papamakarios et al., 2021) is that we have added ψ to the conditioner. The map (2) yields a diffeomorphism $T(\epsilon; \lambda, \psi)$ and defines a ψ -dependent density

$$q(\theta; \lambda, \psi) = q(\epsilon) |\det(J_T(\epsilon; \lambda, \psi))|^{-1} \Big|_{\epsilon=T^{-1}(\theta; \lambda, \psi)},$$

with Jacobian

$$J_T(\epsilon; \lambda, \psi) = \frac{\partial T(\epsilon; \lambda, \psi)}{\partial \epsilon^T}.$$

Here $\epsilon_{<i}$ and ψ are conditioner inputs. For example, if c_i is a MLP then its inputs are $\epsilon_{<i}$ and ψ and λ_i are the network weights and biases. However, when we write $q(\theta|\lambda, \psi)$ or $T(\epsilon; \lambda, \psi)$ we have random variables θ and ϵ while λ and ψ group together as fixed parameters of the density q or map T .

3.2 Amortised objective

We first suppose that prior elicitation has restricted plausible values of ψ to some “focus region” in the space of hyperparameters. We further assume this region has the simple form $\psi_i \in [\tilde{a}_i, \tilde{b}_i]$, $i = 1, \dots, d_\psi$. Some parts of Ψ are of greater interest than others and this is expressed by a “focus density” $\rho(\psi) > 0$, $\psi \in \Psi$. This density determines where we concentrate our effort in finding an accurate variational approximation. In order to get a loss for λ -selection we average the KL-divergence over values of ψ , setting

$$\mathbb{E}_{\psi \sim \rho} [D_{KL}(q(\theta; \lambda, \psi) || p(\theta|Y, \psi))] = \overline{\text{ELBO}}(\lambda) + \log(p(Y)) \quad (3)$$

where $p(Y) = \mathbb{E}_{\psi \sim \rho}(p(Y|\psi))$ and the amortised ELBO is

$$\overline{\text{ELBO}}(\lambda) = \mathbb{E}_{\psi \sim \rho} [\text{ELBO}(\lambda, \psi)] \quad (4)$$

where the ELBO now has additional ψ -dependence in q ,

$$\text{ELBO}(\lambda, \psi) = \mathbb{E}_{\theta \sim q(\theta; \lambda, \psi)} \left[\log \frac{p(\theta, Y | \psi)}{q(\theta; \lambda, \psi)} \right]. \quad (5)$$

The optimal flow parameters are

$$\lambda^* = \arg \max_{\lambda} \overline{\text{ELBO}}(\lambda). \quad (6)$$

See Supplement Section A for how this is computed in the non-amortised case.

This sort of “amortised” setup is commonly used to amortise over data. In that setting the outer expectation is over the prior predictive $y \sim p(\cdot)$ and the user seeks a variational approximation at each value of the data $Y \in \mathcal{Y}$. In contrast we seek an approximation at each hyperparameter value $\psi \in \Psi$. We say that we are “amortising over the hyperparameter”. The two problems share several features. These are well known in the data-amortisation literature. Suppose the variational family *can* express the target distribution with a single λ^* for each ψ . We certainly minimise an integral by minimising the integrand at every point, and we can make the KL-divergence zero at each ψ , so in that idealised setting the optimal λ^* would not depend on the amortisation density ρ . Similar observations are made in Golinski et al. (2019) in the context of data-amortisation. In practice our use of a small number of stacked coupling layer conditioners limits the expressive power of the flow and this leads to ρ -dependence of λ^* . There is an “amortisation gap” (Wu et al., 2020; Margossian and Blei, 2023), the difference in quality of approximation between approximating at all $\psi \in \Psi$ and fitting an approximation at each ψ separately. We investigate this in our experiments and find that we pay very little in quality-of-fit for the gains we make by amortising.

The fitted VMP is most accurate in regions of Ψ where $\rho(\psi)$ is largest, as the empirical estimate for ELBO in (4) is dominated by samples in these regions. Although ρ will in general be arrived at by a process like prior elicitation, it plays a qualitatively different role (and has no influence at all for a universal approximator) so we can use the data to inform it. In this paper we made some initial experiments, which we do not report, to find a “sensible” ρ which covers a priori plausible hyperparameter values with support from the data.

3.3 An amortised universal approximator

For common choices of τ and c_i , $i = 1, \dots, p$, a single autoregressive flow can approximate any given target density $p(\theta|Y, \psi)$ with arbitrary precision by taking increasingly general transformer and conditioner functions (Huang et al., 2018; Papamakarios et al., 2021). We now extend this to the amortised setting.

Denote by $(\mathbb{T}, \mathbb{C}, \mathbb{L})$ a class of autoregressive flows. For example, \mathbb{T} might be the class of all rational quadratic splines on $[0, 1]$, \mathbb{C} the class of all MLPs with any number of inputs and outputs and \mathbb{L} the set of all real vectors with an arbitrary number of elements. A given autoregressive flow (τ, c, λ) belongs to the class if $\tau \in \mathbb{T}$, $c \in \mathbb{C}$ and

$\lambda \in \lambda$. In order to be a well defined flow, λ and ψ must parameterise c and c must parameterise τ , so dimensions match.

Let \mathcal{D} be the class of all probability densities which are continuous and strictly positive on some bounded rectangular region $\Omega = \Omega_1 \times \dots \times \Omega_d$ of \mathbb{R}^d and suppose $\pi \in \mathcal{D}$. Write π as a telescoping product of conditionals,

$$\pi(\omega) = \prod_{i=1}^d \pi(\omega_i | \omega_{<i}) \quad (7)$$

where $\omega_{<i} \in \Omega_{<i}$ where $\Omega_{<i} = \Omega_1 \times \dots \times \Omega_{i-1}$. The map in (2) is invertible. For $i = 2, \dots, p$ let $\epsilon_{<i}(\omega_{<i})$ be given by inversion.

Definition 3.1. A given class of autoregressive flows $(\mathbb{T}, \mathbb{C}, \mathbb{L})$ is a *universal approximator* for distributions in \mathcal{D} if for each $\pi \in \mathcal{D}$ there exists a sequence of flows $\tau^{(k)} \in \mathbb{T}, c^{(k)} \in \mathbb{C}, \lambda^{(k)} \in \mathbb{L}, k \geq 1$ such that for any $\omega_{<i} \in \Omega_{<i}$

$$\omega_i^{(k)} = \tau^{(k)}(\epsilon_i; c_i^{(k)}(\epsilon_{<i}(\omega_{<i}); \lambda_i^{(k)})), \quad i = 1, \dots, p,$$

then $\omega_i^{(k)} \xrightarrow{D} \pi(\cdot | \omega_{<i})$ where D denotes convergence in distribution.

The requirement that Ω is a bounded rectangular region and that π is continuous and strictly positive on Ω is made to connect with Huang et al. (2018). They show that Autoregressive Deep Sigmoidal Flows are a universal approximator for distributions in \mathcal{D} , so there do exist at least some flows satisfying these conditions. See Section A.2 in the supplement for details and Papamakarios et al. (2021) for discussion of related results and further work.

We now give the amortised version. The proof is given in Section B.

Theorem 3.2. Let $\omega = (\psi, \theta)$ be a $d = d_\psi + p$ -dimensional continuous random variable with a probability density $\pi(\omega) = \rho(\psi) p(\theta | Y, \psi)$ which is continuous and strictly positive on a bounded rectangular region $\Omega = \Psi \times \Theta$ of $\mathbb{R}^{-d_\psi + p}$ and let $(\mathbb{T}, \mathbb{C}, \mathbb{L})$ be a class of autoregressive flows satisfying Definition 3.1. There exists a sequence of flows $(\tau^{(k)}, c^{(k)}, \lambda^{(k)})$ (not depending on ψ) such that for all $(\psi, \theta_{<i}) \in \Psi \times \Theta_{<i}$ the transformed random variables

$$\theta_i^{(k)} = \tau^{(k)}(\epsilon_i, c_i^{(k)}(\epsilon_{<i}(\theta_{<i}, \psi), \psi; \lambda_i^{(k)})), \quad i = 1, \dots, p,$$

satisfy $\theta_i^{(k)} \xrightarrow{D} p(\cdot | Y, \theta_{<i}, \psi)$ as $k \rightarrow \infty$ (where $\epsilon_{<i}(\theta_{<i}, \psi)$ is given by inversion of (2)).

The idea of amortising over a hyperparameter appears in Carmona and Nicholls (2022) and Carmona et al. (2024) where the authors amortise over a scalar learning rate η in a generalised Bayes setting. However, they take as their conditioner the form

$$h_i = c_i^{(1)}(\epsilon_{<i}; \lambda_i^{(1)}) + c_i^{(2)}(\psi; \lambda_i^{(2)}) \quad (8)$$

where we take

$$h_i = c_i(\epsilon_{<i}, \psi; \lambda_i). \quad (9)$$

The additive conditioner has many more variational parameters (due to the different structure of the MLP layers in the flow conditioner). It drops co-dependence between ψ and $\epsilon_{<i}$ and will not give a universal approximator. In the examples we looked at this made no practical difference.

4 Hyperparameter selection

The VMP allows us to produce posterior samples for any given set of hyperparameters ψ in an efficient manner, taking $\epsilon \sim q$ and setting $\theta = T(\epsilon; \lambda^*, \psi)$. We can thus select the ψ^* that optimises a suitable loss, leveraging on easy access to the estimated posterior. The choice of loss will depend on the aims of the inference and other details of the data. In the following we give examples of loss functions which are natural in some settings.

When the model is well specified, we can follow [Rezende and Mohamed \(2015\)](#) and choose ψ^* to maximize the ELBO in (1). The ELBO is a good approximation to the marginal likelihood $p(y|\psi)$ when the fitted VMP $q(\theta; \hat{\lambda}^*, \psi)$ is close to the target $p(\theta|Y, \psi)$, and the marginal likelihood is a valid utility in the well specified setting. [Rezende and Mohamed \(2015\)](#) and later authors make a joint maximisation of the ELBO over ψ and λ to estimate λ^* and ψ^* . We need the VMP itself, as a function of ψ , for sensitivity analysis. We fit the VMP and form an estimate $\hat{\lambda}^*$ for λ^* in (6). This gives a posterior approximation at each ψ . If we want a point estimate for ψ we use the fitted VMP to estimate the ELBO at any ψ -value,

$$\widehat{\text{ELBO}}(\hat{\lambda}^*, \psi) = \frac{1}{N} \sum_{i=1}^N \log \left(\frac{p(T(\epsilon^{(i)}; \hat{\lambda}^*, \psi), Y|\psi)}{q(\epsilon^{(i)}) \left| \det(J_T(\epsilon^{(i)}; \hat{\lambda}^*, \psi)) \right|^{-1}} \right) \quad (10)$$

where $\epsilon^{(i)} \sim q(\cdot)$, $i = 1, \dots, N$ are independent samples from the base distribution of the amortised flow. If we trust the marginal likelihood as an estimation criterion, and the ELBO as an estimator, then we set

$$\hat{\psi}^* = \underset{\psi}{\operatorname{argmax}} \widehat{\text{ELBO}}(\lambda^*, \psi).$$

When the model is not well-specified and the goal of the inference is prediction then we use a loss based on predictive performance on held out data. In our examples we use the Expected Log Pointwise Predictive Density (ELPD) for new data ([Vehtari et al., 2017](#)) as the criterion. The idea of using the ELPD to select the learning rate in a Generalised Bayes setting was suggested in [Carmona and Nicholls \(2020\)](#) (who estimate the ELPD using the WAIC, ([Watanabe, 2010](#))). In that setting the loss for ψ is

$$\mathcal{L}(\psi) = - \int p^*(y') \log(p(y'|y; \psi)) dy'$$

where p^* is the true generative model for the data and $p(y'|y; \psi)$ is the posterior predictive distribution for one component of new data (hence ‘‘pointwise’’). [McLatchie et al.](#)

(2024) observe that, when η is not close to zero and the data size is moderately large, the ELPD is insensitive to η . In contrast, here and in Carmona and Nicholls (2020) and Carmona and Nicholls (2022) we see significant dependence and a clear maximum. This may be due to the data-to-parameter dimension scaling. In our examples, the dimension of the parameter space increases as the number of observations increases: this is outside the setting considered in McLatchie et al. (2024). Cooper et al. (2024) show that the ELPD can perform poorly when there is serial dependence across components of the data, so the ELPD should be used with care.

We estimate the ELPD using the data and our variational approximation writing

$$\widehat{p(y'|y; \psi)} = \mathbb{E}_{\theta \sim q(\cdot; \widehat{x}, \psi)}(p(y'|\theta)).$$

The LOOCV estimator for the (negative) ELPD is then

$$\hat{\mathcal{L}}(\psi) = - \sum_{i=1}^n \log \left(\widehat{p(y_i|y_{-i}; \psi)} \right) \quad (11)$$

where y_{-i} is the data with the i 'th sample removed, and we set $\hat{\psi}^* = \operatorname{argmin}_{\psi} \hat{\mathcal{L}}(\psi)$. We used LOOCV rather than WAIC as we expect LOOCV to be more reliable than WAIC on the small dataset we analyse in Section 6.2.

If the goal of the inference is parameter estimation then the square-loss to the true parameter value may be ideal, but unavailable. One generic setting where we can access this loss arises when the parameters we wish to estimate are physical quantities X_i , $i \in \mathcal{P}$ which are present and interpretable whether or not the model is misspecified. Consider a model of the form

$$\begin{aligned} \alpha &\sim p(\alpha; \psi), \\ X_i &\sim p(\cdot; \psi), \\ Y_i &\sim p(\cdot|X_i, \alpha; \psi), \end{aligned} \quad (12)$$

jointly independent for $i \in \mathcal{P}$. Suppose some subset $A \subset \mathcal{P}$ of the X 's are perfectly observed (the ‘anchors’) so that $X_a = x_a$ is given for $a \in A$ and the values of X_m , $m \in M$, $M = \mathcal{P} \setminus A$ are missing. The posterior of interest is

$$p(\alpha, X_M | y_{\mathcal{P}}, x_A; \psi) \propto p(\alpha; \psi) \prod_{m \in M} p(y_m | \alpha, X_m; \psi) p(X_m; \psi) \prod_{a \in A} p(y_a | \alpha, x_a; \psi) p(x_a; \psi). \quad (13)$$

Denote by x_m the unknown true value of X_m , $m \in M$. We would like to target the Posterior Mean Squared Error

$$\text{PMSE}(\psi) = \frac{1}{|M|} \sum_{m \in M} \mathbb{E}_{\alpha, X_m} (||x_m - X_m||^2 | y_{\mathcal{P}}, x_A; \psi)$$

and set $\psi^* = \operatorname{argmin}_\psi \operatorname{PMSE}(\psi)$ but x_M is unknown. However, if the pairs $(X_i, Y_i)_{i \in \mathcal{P}}$ are exchangeable, we can target a cross-validated objective, holding out a subset $B \subset A$ of anchors and computing

$$\widehat{\operatorname{PMSE}}_{LMO}(\psi) = \frac{1}{|B|} \sum_{a \in B} \mathbb{E}_{\alpha, X_a} (\|x_a - X_a\|^2 | y_{\mathcal{P}}, x_{A \setminus B}; \psi), \quad (14)$$

and setting $\hat{\psi}^* = \operatorname{argmin}_\psi \widehat{\operatorname{PMSE}}_{LMO}(\psi)$. In (14) we treat the labels with indices in B just as if they were more missing labels alongside M , so the VMP we use to estimate the expectation in (14) is $q(\alpha, X_B, X_M; \hat{\lambda}^*, \psi)$.

5 The VMP for Semi-Modular Inference

The VMP is appealing for the tuning of any hyperparameter that is relevant to posterior estimation. So far, we have focused on *model* hyperparameters. However, we may be interested in hyperparameters of the *inference* such as the *learning rate* in GBI (GBI, Bissiri et al. (2016); Grünwald and Ommen (2017)). In GBI the negative log likelihood is replaced by a loss which need not determine a normalisable likelihood (Jewson and Rossell, 2022). This degree of freedom can be helpful for treating misspecification. The learning rate weights the loss relative to the prior. The loss itself may have hyperparameters. These can all be treated in the same way as model-hyperparameters in the VMP framework. In fact, the VMP was developed to estimate the learning rate in the context of Semi-Modular Inference (SMI, Carmona and Nicholls (2020)), a variant of GBI useful for working with multiple data sets. Estimation of inference hyperparameters “selects the belief update”. For example, the β -loss has an inference hyperparameter β and estimation methods date back to Warwick and Jones (2005). See Jewson et al. (2024) for recent review. For recent developments and reviews of learning rate estimation see (Wu and Martin, 2023; Winter et al., 2023).

Here we give a very brief outline of SMI and the VMP for SMI, and refer the reader to Carmona and Nicholls (2022) for further detail. Our contribution is to use the VMP to estimate learning rates and model hyperparameters jointly.

5.1 Semi-Modular Inference (SMI)

SMI (Carmona and Nicholls, 2020) is a form of Bayesian Multiple Imputation that is useful when we have several data sets with generative models or “modules” which share “extrinsic” parameters. We illustrate SMI in the context of a generative model with two modules, $\{Z, \delta\}$ and $\{Y, \theta, \delta\}$ which share a model parameter δ :

$$\delta \sim p(\delta; \psi), \quad (15)$$

$$Z \sim p(Z|\delta), \quad (16)$$

$$\theta \sim p(\theta|\delta; \psi), \quad (17)$$

$$Y \sim p(Y|\theta, \delta), \quad (18)$$

prior hyperparameters ψ , data $Y = (Y_1, \dots, Y_n)$ and $Z = (Z_1, \dots, Z_m)$ and posterior

$$p(\delta, \theta | Z, Y; \psi) = p(\delta | Z, Y; \psi) \times p(\theta | \delta, Y; \psi), \quad (19)$$

Equation (19) gives the standard Bayesian posterior in a factorisation relevant for Bayesian Multiple Imputation (Meng, 1994): δ is “imputed” via the marginal $p(\delta | Z, Y; \psi)$ (integrated over θ) at the first stage and passed to the second stage where we “analyse” θ via the conditional $p(\theta | \delta, Y; \psi)$.

Suppose the Y-module is misspecified. SMI tempers information from Y in the imputation of δ using an auxiliary copy of the variable $\tilde{\theta}$ and a learning rate $\eta \in [0, 1]$,

$$p_{smi}(\delta, \theta, \tilde{\theta} | Y, Z; \tilde{\psi}) \equiv p_{pow}(\delta, \tilde{\theta} | Y, Z; \tilde{\psi}) p(\theta | \delta, Y; \psi) \quad (20)$$

where $\tilde{\psi} = \{\eta, \psi\}$ and

$$p_{pow}(\delta, \tilde{\theta} | Y, Z; \tilde{\psi}) \equiv \frac{p(Z | \delta) p(Y | \delta, \tilde{\theta})^\eta p(\delta, \tilde{\theta}; \psi)}{p(Z, Y; \eta)}. \quad (21)$$

When we impute δ using $p_{pow}(\delta, \tilde{\theta} | Y, Z; \tilde{\psi})$, an auxiliary “copy” of θ is needed in order to access information from the likelihood $p(Y | \delta, \tilde{\theta})$. The learning rate η dials down the flow of information from $p(Y | \delta, \tilde{\theta})$ into δ . When $\eta = 1$ the marginal for δ, θ is the posterior in (19). When $\eta = 0$, information from Y is cut (Lunn et al., 2009; Plummer, 2015) and δ is imputed from Z alone. Asymptotic behavior of SMI is set out in Frazier and Nott (2023b) and Frazier and Nott (2023a).

5.2 VMP for SMI

The VMP is particularly suitable for inference targeting the SMI posterior in (20). The parameterisation and target loss are designed to ensure the same control of information flow built into the SMI belief update holds in the VMP also. Yu et al. (2023) use a similar approach to fit a variational approximation to the cut-posterior. We take a simple base distribution $p(\epsilon_1)$ for the flow for δ and matching base distributions $p(\epsilon_2 | \epsilon_1)$ and $p(\epsilon_3 | \epsilon_1)$ for the conditional θ and $\tilde{\theta}$ distributions, with $\dim(\epsilon_1) = \dim(\delta)$ and $\dim(\epsilon_2) = \dim(\epsilon_3) = \dim(\theta) = \dim(\tilde{\theta})$ and consider a variational approximation parametrised by NFs of the form

$$\begin{aligned} q(\theta, \tilde{\theta}, \delta; \lambda, \tilde{\psi}) &= q_1(\delta; \lambda_1, \tilde{\psi}) q_2(\theta; \delta; \lambda_2, \tilde{\psi}) q_3(\tilde{\theta}; \delta, \lambda_3, \tilde{\psi}) \\ &= p(\epsilon_1) |J_{T_1}|^{-1} p(\epsilon_2 | \epsilon_1) |J_{T_2}|^{-1} p(\epsilon_3 | \epsilon_1) |J_{T_2}|^{-1} \end{aligned} \quad (22)$$

where T_1, T_2 and T_3 are normalising flows with flow parameters $\lambda = \{\lambda_1, \lambda_2, \lambda_3\}$. This allows us to enforce the conditional independence structure that we are assuming in the model and control each NF separately.

As explained in Carmona and Nicholls (2022) and Yu et al. (2023), flow-fitting must be done in two stages in order to stop the variational approximation from introducing uncontrolled information flow between modules. See Section C for the main idea and the cited papers for detail.

6 Experiments

We consider three datasets: a simple synthetic dataset in Section 6.1 simulated from a hierarchical model, analysed in a standard Bayesian framework with a well-specified prior and likelihood and hyperparameters estimated using the ELBO; the well known HPV data in Section 6.2 analysed in an SMI setting with hyperparameters estimated using the ELPD; and a dataset of Linguistic Profiles (LP, Section 6.3) also analysed in an SMI setting but now hyperparameters are estimated using the PMSE. We focus on hyperparameters which are reasonably well-informed by the data. These hyperparameters control priors for groups of exchangeable parameters. Each parameter replicate is informed by the data, and this ultimately informs the hyperparameter.

Our main interest is in the quality of the posterior approximation provided by the VMP $q(\theta; \lambda^*, \psi)$ and how well it informs ψ when we use the criteria (ELBO, ELPD, PMSE) in Section 4 to learn about ψ . We have two baselines of increasing quality and cost: we compare the VMP against VP densities fitted separately at each ψ ; we compare against MCMC (for the LP data we found MCMC too computationally expensive to be workable for the full dataset so in that case we benchmark on a subset of the data).

6.1 Synthetic Data

We first consider synthetic data and standard Bayesian inference with no model misspecification. We use the fitted VMP to estimate hyperparameters and check they match true values. The data generating process for the random effects model is

$$\begin{aligned} \mu_j &\sim N(m, s^2) \\ \sigma_j &\sim \text{IG}(g_1, g_2), \quad j = 1, \dots, J \\ Y_{ij} &\sim N(\mu_j, \sigma_j), \quad i = 1, \dots, I. \end{aligned} \tag{23}$$

with hyperparameters $\psi = (m, s^2, g_1, g_2)$, true values $\psi_{True} = (0, 1, 1.5, 0.5)$ and IG the Inverse Gamma distribution with shape g_1 and scale g_2 .

When I and J are large, hyperparameter estimation is “easy”: the hyperparameters each control the distribution of J exchangeable parameters which are informed directly from the data. The VMP is trained by maximising $\overline{\text{ELBO}}$ in (4) under the true generative model in (23). The hyperparameter distribution ρ used for amortisation were Normal(0, 3) (for μ), Gamma(shape=2, scale=1) (for σ) and Gamma(0.5, 2) (for both g_1 and g_2). Once we have estimated λ^* we select hyperparameters by maximising the ELBO-estimator in (10) as a proxy for maximising $p(Y|\psi)$.

We consider a small dataset where $I = 8$ and $J = 10$ and a larger dataset where $I = 50$ and $J = 50$. Training loss and hyperparameter trace plots from the second-stage ψ -optimisation are shown in Figure 6 (small data set) and Figure 8 (large data set) of Appendix E.1 in the Supplementary Material (Battaglia and Nicholls, 2024). In Table 1 we give the hyperparameter values which maximise $\widehat{\text{ELBO}}(\lambda^*, \psi)$. For the large dataset these are very close to the true values. In Figures 9 and 10 of Appendix E.1 we plot the posteriors we estimate for μ and σ on the large data set using three different

methods: MCMC at the true values ψ_{True} (the oracle); the VP fitted at ψ_{True} ; the VMP posterior at hyperparameters ψ^* estimated using the VMP. These are all essentially indistinguishable. On the small dataset, estimated hyperparameter values in Table 1 differ a bit more from true values and the difference in the reconstructed posteriors is visible in Figures 1, though slight. There is little under-dispersion (despite the reverse-KL) due to the relatively simple target and the expressive power of a normalising flow.

	True Value	Estimated Optimum	
		Small	Large
m	0.0	0.4	0.01
s	1.0	0.85	0.98
g_1	1.5	1.05	1.42
g_2	0.5	0.43	0.5

Table 1: True vs VMP-estimated optimal values for the synthetic dataset where $I = 8$ and $J = 10$ (small dataset) and that where $I = 50$ and $J = 50$ (large dataset).

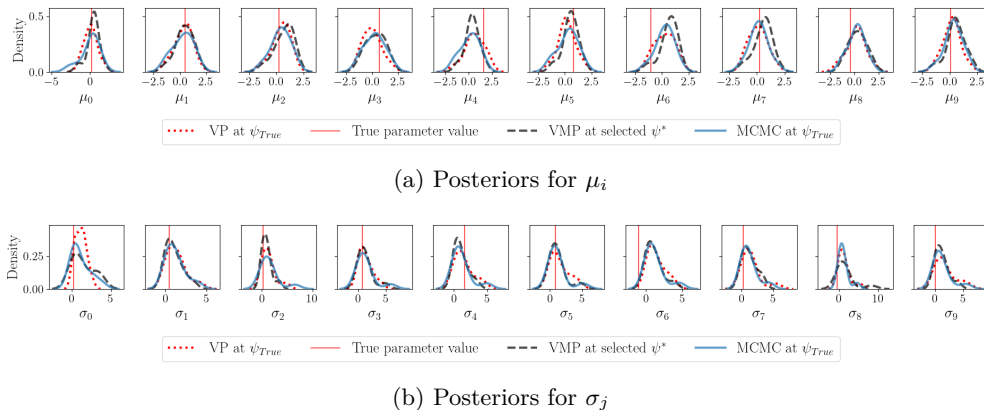


Figure 1: Synthetic small dataset. Ground truth posteriors compared to VMP posteriors at selected hyperparameters. See Figures 9 and 10 for the large data set.

6.2 HPV data

6.2.1 Model and data

In this section we give an example targeting the LOOCV estimator for the ELPD to estimate $\tilde{\psi}^*$ for an epidemiological model analysed in Plummer (2015) and based on data from human papillomavirus (HPV) prevalence surveys and cancer registries for age group cohorts (55-64 years) over $n = 13$ countries (Maucort-Boulch et al., 2008). Outcome Y_i denotes the count of cancer instances observed over T_i woman-years of

monitoring in the i -th country, while Z_i indicates the number of high-risk HPV instances identified in a sample comprising N_i women from the same population. The model has a Poisson module for cancer incidence and a Binomial module for HPV prevalence,

$$\begin{aligned} Z_i &\sim \text{Binomial}(N_i, \delta_i), \\ Y_i &\sim \text{Poisson}(\mu_i), \\ \mu_i &= T_i \exp(\theta_1 + \theta_2 \delta_i), \end{aligned} \tag{24}$$

for $i = 1, \dots, n$ with priors

$$\begin{aligned} \delta_i &\sim \text{Beta}(c_1, c_2) \\ \theta_1 &\sim N(m, s^2) \\ \theta_2 &\sim \text{Gamma}(g_1, g_2). \end{aligned}$$

The model for the survey data Z is well specified but cancer incidence Y is misspecified.

6.2.2 SMI with the VMP and amortised prior hyperparameters

In this section we fit the VMP of Section 5.2 to the SMI-posterior in (20) for the case of the generative model in (24). The VMP approximates the posterior for θ and δ . It is amortised over c_1, c_2 and η with hyperparameters m, s, g_1, g_2 fixed to 0, 100, 1, 0.1 respectively. We could learn a VMP for all the hyperparameters and carry out a sensitivity analysis. However, the data informs them weakly, as they control a single parameter. Working with fixed c_1, c_2 , Carmona and Nicholls (2020) found that the WAIC selects $\eta = 1$ (Bayes) when targeting prediction of Y , while $\eta = 0$ (Cut-posterior) was preferred for Z . We get similar results for η . In Section E.2.1 in the Supplementary Material we repeat this analysis for Bayesian inference with $\eta = 1$ fixed.

We fit the VMP by estimating λ^* using the amortised ELBO-measures determined by the divergences in (32) and (33). We amortise over η, c_1 and c_2 using ρ -distributions $c_1, c_2 \sim \text{Uniform}(0, 15)$ $\eta \sim \text{Uniform}(0, 1)$. We arrived at this after some experiments which we omit, aiming for support on all a priori plausible hyperparameter values. We then estimate $\tilde{\psi}^*$ by minimising $\hat{\mathcal{L}}(\tilde{\psi})$ in (11), using the Y or Z data depending on which ELPD we target. The optimisation traces are shown in Figure 13 in the Supplementary Material. The SGD can get stuck at sub-optimal values so we take the hyperparameters achieving the least loss over multiple SGD-initialisations. This gives $\tilde{\psi}_Y^* = \{0.87, 13.04, 15\}$ when targeting Y , and $\tilde{\psi}_Z^* = \{0.02, 0.97, 14\}$ when targeting Z , in line with earlier work (Cut for Z and Bayes for Y). Hyperparameters η and c_1 are well-informed by the data. For c_2 we simply learn that large values are favored.

The posterior is sensitive to the choice of hyperparameters. This is illustrated in Figure 2, which shows samples for θ at $\eta = 0.87$ (blue) and $\eta = 0.02$ (orange) at the optimal c_1 and c_2 values. The univariate densities along the two axes show variation in the posterior for θ if we vary c_1 and c_2 keeping η fixed. The overlaid KDE contours for MCMC samples targeting the SMI posterior at $\tilde{\psi}_Y^*$ and $\tilde{\psi}_Z^*$ agree with the VMP samples. On the Y -module, the optimal $\tilde{\psi}_Y^*$ values lie at the boundary of the support

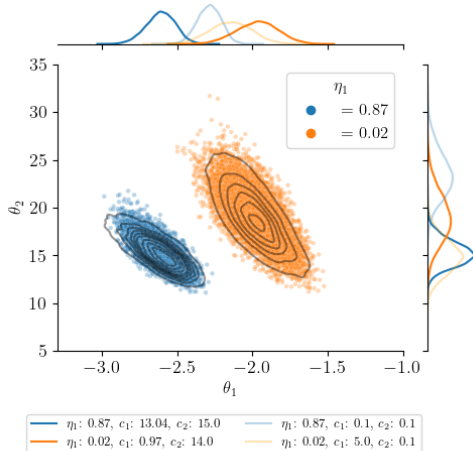


Figure 2: SMI analysis of HPV data. VMP samples for θ_1 and θ_2 at $\eta = 0.87$ (blue) and $\eta = 0.02$ (orange) at optimal (full opacity) and alternative (reduced opacity) prior hyperparameters; overlaid with KDE contours for corresponding MCMC distributions.

of the ρ -distribution where the VMP has few training samples. This can be resolved by adjusting the ρ -distribution. In a real VMP application we wouldn't have the MCMC benchmark so we have left this unadjusted.

Figures 14a and 14b in Section E.2 show distributions for selected δ_i 's at $\eta = 0.87$ and $\eta = 0.02$ respectively. Although these posterior distributions are sensitive to c_1 and c_2 , the VMP is able to follow the dependence and VMP approximations match MCMC distributions very well.

6.3 Linguistic Profile data

6.3.1 Background to the data

In this section we illustrate hyperparameter estimation using the VMP to target the PMSE's. Carmona et al. (2024) estimates latent spatial frequency fields for late-medieval English dialect word forms from 1350CE-1450CE. The data are 367 "Linguistic Profiles" (LPs) recording the presence and absence of 741 dialect spellings and grammatical forms across 367 documents from a 200km x 180km region in central Great Britain which we rescale to $\mathcal{X} = [0, 1] \times [0, 0.9]$. These data are a subset of the Linguistic Atlas of Late Medieval English (LALME) (McIntosh et al., 1986), originally including 1044 LPs from text samples written in England, part of Wales and southern Scotland. Each LP records the presence ($y_{p,i,f} = 1$) or absence ($y_{p,i,f} = 0$) of a form $f \in \mathcal{F}_i$ for an item $i \in \mathcal{I}$ in document $p \in \mathcal{P}$, across all 367 LPs (in fact somewhat more information is available). For example, the singular noun "brother" is an item, with distinct forms including "BROTHER", "BROTHER", "BROyer", "BROyEr", "BROTBYR" and "BRUTHIR"

(Haines (2016) and note “E” and “e” etc represent different letters in the manuscripts, not a change of case) and any given document will only contain one or two of these forms (if the item is used at all).

Among the 367 LPs, 120 have precise location data ($x_p \in \mathcal{X}$, $p \in A$). The remaining 247 LPs have missing locations $x_p \in \mathcal{X}$, $p \in M$ (with $\mathcal{P} = A \cup M$). The Atlas authors call profiles in A and M the *anchor* and *floating* profiles. They provide estimates for the locations of the floating profiles. A map of the locations of the LPs can be found in Section E.3 of the supplement. In our subset of the Atlas data we have 71 items so $\mathcal{I} = \{1, 2, \dots, 71\}$. The present analysis re-estimates the locations of the floating LPs and compares them to the values given by the Atlas authors. When we estimate a location for a floating profile we expect it to be placed in a region where the dialect forms it contains appear frequently.

6.3.2 Background to the model

Haines (2016) introduces these data in a statistical setting and gives a statistical framework to simultaneously estimate latent spatial fields for the incidence-frequencies of forms and estimate the missing locations of the floating LPs. Details of the model are set out in Section E.3.1 in the supplement. We give a brief summary here. In a document a given item is used a Poisson number of times with item-dependent mean μ_i . Given item i is used it takes form $f \in \mathcal{F}_i$ with a location-dependent form-usage probability $\phi_{i,f}(x_p)$ satisfying $\sum_{f \in \mathcal{F}_i} \phi_{i,f}(x_p) = 1$. The binary data $y_p = (y_{p,i,f})_{f \in \mathcal{F}_i}^{i \in \mathcal{I}}$ for profile $p \in \mathcal{P}$ at location x_p are generated by taking independent Poisson random variables $z_{p,i,f}$ with mean $\mu_i \phi_{i,f}(x_p)$, zero-inflating them with independent Bernoulli variables $z'_{p,i,f} \sim \text{Bernoulli}(1 - \zeta_i)$ and thresholding them, so that $y_{p,i,f} = \mathbb{I}_{z'_{p,i,f} z_{p,i,f} > 0}$. Here ζ_i is the item-dependent zero-inflation probability.

Denote by $\Phi(x) = (\phi_{i,f}(x))_{f \in \mathcal{F}_i}^{i \in \mathcal{I}}$ the multi-dimensional latent spatial form-frequency field $\Phi : \mathcal{X} \rightarrow [0, 1]^{d_\Phi}$, $d_\Phi = \sum_{i=1}^I |\mathcal{F}_i| = 741$ at a generic location $x \in \mathcal{X}$. Haines (2016) gives a prior for Φ which proved to be misspecified. Carmona et al. (2024) gave the following improved model for Φ . In order to reduce the dimensionality of the problem and induce correlation across items and forms at a given location, they parametrise the fields as a (soft-maxed) linear combination of a small number of shared basis fields $\gamma_b : \mathcal{X} \rightarrow \mathbb{R}$, $b = 1, \dots, B$, taking B equal to 10. To induce correlation across locations, the basis fields are modeled as Gaussian Processes (GPs) with a common kernel $k(\cdot, \cdot)$ modeling spatial decay of correlation.

$$\begin{aligned} \phi_{i,f}(x_p) &= \frac{\exp(\gamma_{i,f}(x_p))}{\sum_{f' \in \mathcal{F}_i} \exp(\gamma_{i,f'}(x_p))} \\ \gamma_{i,f}(x_p) &= a_{i,f} + \sum_{b=1}^B \gamma_b(x_p) w_{i,f,b} \\ \gamma_b(x_p) &\sim GP(0, k(\cdot, \cdot)) \quad b \in \mathcal{B} = \{1, \dots, B\} \end{aligned}$$

The kernel $k(\cdot, \cdot)$ is an exponential kernel with amplitude σ_k and length-scale ℓ_k . Denote by $\alpha = (\mu, \zeta, a, W)$ the parameters μ, ζ for the zero-inflated Poisson observation model,

the weights $W = \{w_{i,f,b}\}$ and their offsets $a = \{a_{i,f}\}$. Let $\Gamma(X_{\mathcal{P}}) = (\gamma_b(x_p))_{b \in \mathcal{B}}^{p \in \mathcal{P}}$ denote the set of GP basis-field values at profile locations (including anchor locations $X_A = (x_p)_{p \in A}$ and the locations $X_M = (x_p)_{p \in M}$ of floating profiles). The prior for X_M is uniform in $\mathcal{X}^{|M|}$. The weights W and offsets a are given zero-centred Laplace and zero-centred Gaussian independent priors with scales σ_w and σ_a respectively. The priors for μ_i, ζ_i $i \in \mathcal{I}$ given in (37) and (38) in Section E.3.1 in the Supplement have no unknown hyperparameters. The full set of hyperparameters we study is $\psi = (\sigma_a, \sigma_w, \sigma_k, \ell_k)$.

The aim of the analysis is to summarise the posterior $p(\alpha, \Gamma(X_{\mathcal{P}}), X_M | Y_{\mathcal{P}}, \psi)$ with particular interest in estimating X_M . Our contribution is to use the VMP to approximate this posterior at a useful range of hyperparameter values ψ , check for sensitivity to the choice of ψ and estimate ψ where feasible. The exact joint distribution given hyperparameters is

$$p(Y_{\mathcal{P}}, \alpha, \Gamma(X_{\mathcal{P}}), X_M | \psi) = p(\alpha | \sigma_a, \sigma_w) p(Y_A | \alpha, \Gamma(X_A)) p(Y_M | \alpha, \Gamma(X_M)) \\ \times p(X_M) p(\Gamma(X_A), \Gamma(X_M) | X_M, \sigma_k, \ell_k) \quad (25)$$

Carmona et al. (2024) go on to make a widely-used approximation, parameterising the GPs at a fixed lattice of 121 inducing-points $\mathcal{U} \subset \mathcal{X}$ rather than at the profile locations and approximating the joint distribution of the GPs at profile locations given the DP values at inducing points. This is convenient for variational work and further reduces the parameter dimension. The final approximate posterior $p(\alpha, \Gamma(X_{\mathcal{U}}), X_M | Y_{\mathcal{P}}, \psi)$ is given in Equation (49) in Section E.3.1 in the supplement.

6.3.3 Tuning hyperparameters for the LALME data

In Section E.3.2 in the supplement we compare the VMP with the VP and MCMC, working with a subset of the LALME data described in Section 6.3.1 so that MCMC is feasible, and targeting the posterior in (49) in supplement Section E.3.1. As in in Sections 6.1 and 6.2, we find that the VMP is able to learn a posterior approximation to the MCMC baseline of similar quality to that provided by the VP. The target distribution is far more complex than the earlier examples but the amortised flow is sufficiently general to express the target.

In this section we use the VMP to estimate hyperparameters for all the LALME data in the study region \mathcal{X} , with 371 profiles observed over 71 items presenting 741 forms. The posterior in (49) is a density over 9997 dimensions, and MCMC is infeasible. See Table 2 in Section E.3 of the supplement for a complete breakdown of parameter dimensions. Furthermore, as Haines (2016) and Carmona et al. (2024) show, the model in Section 6.3.2 is misspecified. These issues motivated Carmona et al. (2024) to apply SMI, using the VMP to estimate η and the locations X_M of floating profiles. Here we show that prior hyperparameters can be treated in the same framework.

Denote by $\tilde{\psi} = \{\psi, \eta\}$ the set of all hyperparameters. The SMI set-up for this example can be set in the same modular structure as (15), taking

$$Z \equiv Y_A, \quad Y \equiv Y_M$$

$$\theta \equiv X_M \qquad \delta \equiv \alpha, \Gamma(X_U).$$

These choices identify the module $\{Y_A, \alpha, \Gamma(X_U)\}$ as well specified and the module $\{Y_M, X_M, \alpha, \Gamma(X_U)\}$ as misspecified, reflecting the fact that anchor-texts and non-anchor texts (ie floating profiles) are somewhat different types of texts. The SMI-posterior replacing the Bayes posterior $p(\alpha, \Gamma(X_U), X_M|Y_{\mathcal{P}}, \psi)$ approximating (25) is

$$p_{smi}(\alpha, \Gamma(X_U), X_M, \tilde{X}_M|Y_{\mathcal{P}}; \tilde{\psi}) \equiv p(X_M|\alpha, \Gamma(X_U), Y_M; \psi) \quad (26) \\ \times p_{pow}(\alpha, \Gamma(X_U), \tilde{X}_M|Y_{\mathcal{P}}; \tilde{\psi})$$

where \tilde{X}_M are the auxiliary parameters introduced in SMI to access information from the observation model for Y in the ‘‘imputation’’ stage. The variational posterior is

$$q(X_M, \tilde{X}_M, \alpha, \Gamma(X_U); \lambda, \tilde{\psi}) = q_1(X_M|\alpha, \Gamma(X_U); \lambda_1, \psi) q_2(\tilde{X}_M|\alpha, \Gamma(X_U); \lambda_2, \tilde{\psi}) \\ \times q_3(\alpha, \Gamma(X_U); \lambda_3, \tilde{\psi}) \quad (27)$$

and we use the VMP as per Section 3 as variational family.

For ρ distributions for $\tilde{\psi}$, we take Gamma(10, 1), Gamma(5, 1), Uniform(0.1, 0.4), Uniform(0.2, 0.5) and Beta(0.5, 0.5) for $\sigma_a, \sigma_w, \sigma_k, \ell_k$ and η respectively. These choices are guided by the same physical considerations we would use to do prior elicitation. For example, we are unlikely to see significant dialect changes in less than 20km but 100km should be enough, translating to a range [0.1, 0.5] for ℓ_k after scaling. Some experiments showed that focusing on [0.2, 0.5] concentrated training on the range of ℓ_k values actually favored by the data. We choose a ρ for η that concentrates on values of η close to 0 and 1, corresponding to strongly or negligibly misspecified. In fact we will see that a moderate η is favored. The VMP performed well despite using a search focus covering but directed away from the optimal value. We estimate λ^* minimising the SMI objectives given in (32) and (33). This gives the fitted VMP $q(X_M, \tilde{X}_M, \alpha, \Gamma(X_U); \lambda^*, \tilde{\psi})$.

The goal of the whole analysis is to estimate the float-locations X_M , so we use the PMSE outlined in Section 4 to select $\tilde{\psi}$. The observed anchor locations X_A are an obvious proxy for the X_M : if we are good at predicting the locations of held out anchors then we will be good at predicting the locations of floating profiles. We take a subset $\mathcal{K} \subset A$ of $K = 40$ randomly chosen anchor profiles and make a single train-test split, leaving $|A| - K = 80$ in the training set. The optimal hyperparameters are given by

$$\hat{\psi}^* = \operatorname{argmin}_{\tilde{\psi}} \mathbb{E}_{X_p \sim \hat{q}_{\tilde{\psi}}^{\text{train}}} \left(\sum_{p \in \mathcal{K}} \|x_p - X_p\|^2 \right) \quad (28)$$

where $x_p, p \in \mathcal{K}$ are the true locations of the held out anchors, X_p are posterior locations for the same quantities, and $\hat{q}_{\tilde{\psi}}^{\text{train}} = q(X_{M \cup \mathcal{K}}, \tilde{X}_{M \cup \mathcal{K}}, \alpha, \Gamma(X_U); \lambda^*, \tilde{\psi})$ is a VMP trained with held-out anchors in \mathcal{K} treated as missing (so X_A becomes $X_{A \setminus \mathcal{K}}$). This is evaluated at ψ and approximates $p_{smi}(\alpha, \Gamma(X_U), X_{M \cup \mathcal{K}}, \tilde{X}_{M \cup \mathcal{K}}|Y_{\mathcal{P}}; \tilde{\psi})$ in (26). We minimise the PMSE in Equation (28) using SGD, taking derivatives over ψ via automatic differentiation.

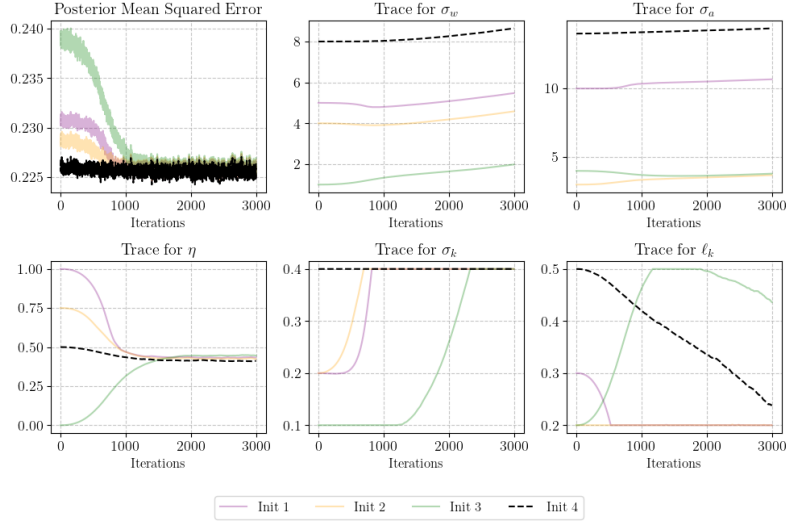


Figure 3: LALME data. Training loss and trace plots for hyperparameter optimisation of each component of ψ at different initialisations. The run achieving the lowest average loss over the last 20 iterations is highlighted in black. Hyperparameters were selected as the average values over the 20 last iterations of this run.

Optimisation traces for four initialisations are shown in Figure 3. The rapidly converging learning rate η drives the decrease in PMSE with $\tilde{\psi}^*$; we estimate $\hat{\eta} = 0.42$. Working with fixed prior hyperparameters ψ , Carmona et al. (2024) estimates $\hat{\eta} = 0.75$; our smaller η removes more information from the Y -module inference for α and $\Gamma(X_U)$, so we find a little more evidence for misspecification when optimising over a larger space. The drop in PMSE after fixing the misspecification corresponds to a root-PMSE gain of 7km in prediction accuracy. The large optimal σ_k and small ℓ_k values in Figure 3 favor GP fields that vary by relatively large amounts over short spatial scales. The PMSE is not sensitive to σ_w and σ_a (different values give the same loss), as long as they are large enough to admit the weights w and biases a for the mixture of Gaussian processes that the data support. Based on this sensitivity analysis, we identify the hyperparameter vector $\psi^* = \{\sigma_a = 10, \sigma_w = 5, \sigma_k = 0.4, \ell_k = 0.2, \eta = 0.42\}$ as suitable.

Figure 4 shows posterior distributions for 21 of the 40 held-out anchor profiles at $\eta = 0, 0.42, 1$, keeping the other hyperparameters ψ fixed at ψ^* . Modulating the information flow from the misspecified Y_M -module via SMI helps for many profiles (distributions shift closer to true values). However, cutting all that information ($\eta = 0$) gives overdispersed results (e.g. profiles 138, 1205); this bias-variance trade-off is behind the gain in PMSE at η somewhere between cut and Bayes. In Figure 19 of Section E.3.4 of the Supplementary Material (Battaglia and Nicholls, 2024) we use the trained VMP at $\tilde{\psi}^*$ to estimate the locations X_M of floating profiles. This was the main goal of the analysis. We show VMP-posterior distributions for 10 randomly selected floating profiles

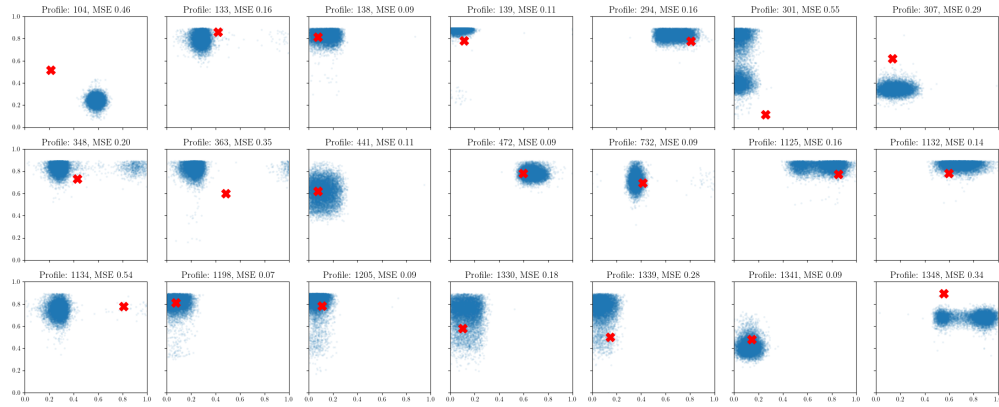
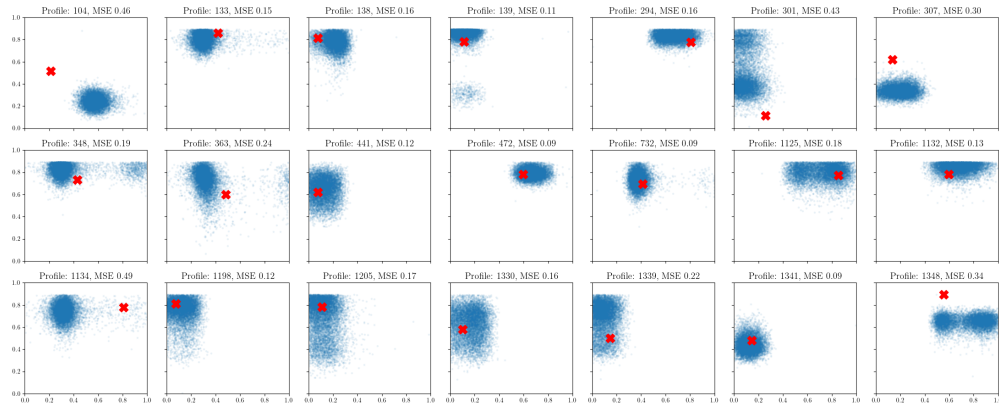
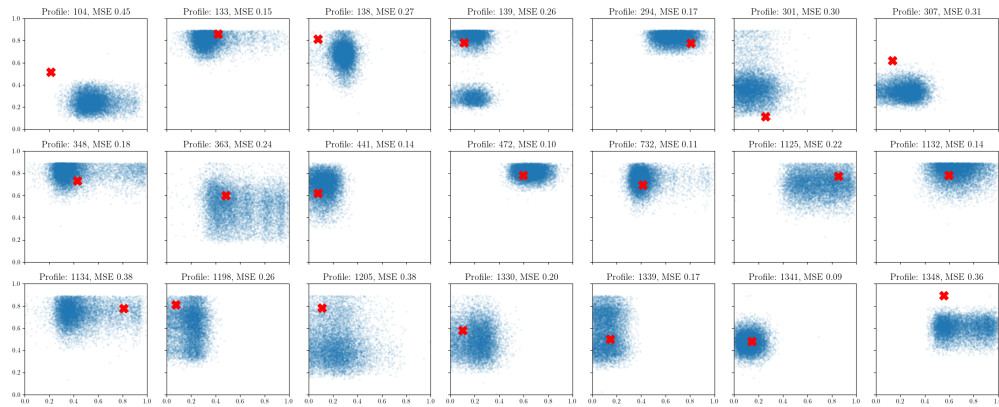
(a) $\eta = 1$ (b) $\eta = 0.42$ (c) $\eta = 0$

Figure 4: LALME data. Posterior distributions of locations for 21 held-out anchor profiles using the VMP at optimal prior hyperparameters $\sigma_a = 5$, $\sigma_w = 10$, $\sigma_k = 0.4$, $\ell_k = 0.2$.

and compare them with the Atlas locations (which are themselves estimates), making use of the trained VMP evaluated at ψ^* . These are simply our original fit with held out anchors; it would be natural to refit a VP at the estimated optimal ψ^* using all the anchors though the gains are small.

Figure 20 shows how the VP training losses (negative SMI-ELBO) of the fitted VP and VMP vary with η ; let $L_{VP}(\eta, \psi)$ and $L_{VMP}(\eta, \psi)$ denote these losses; we might expect $L_{VP}(\eta; \psi) < L_{VMP}(\eta; \psi)$ (an amortisation gap) as the ‘‘local’’ VP fits at fixed η, ψ while the VMP is one fit at all η, ψ . We find the gap is too small to measure. See Section E.3.4 in the supplement for further detail.

7 Conclusions

We have set out a variational framework for exploring posterior hyperparameter dependence by fitting a normalising flow amortised over hyperparameter values. The fitted VMP can be used to check for sensitivity to the choice of hyperparameters or to estimate hyperparameters by minimising a suitable loss. The posterior mean square error for parameter estimates is particularly well suited when it is available (as it was in the example in Section 6.3).

Classical methods may be used in hyperparameter sensitivity-analysis. However, they are very slow by comparison with the VMP. In Section F in the Supplement we give implementation details for our VMP and run times for all experiments. Quantitative comparison between the VMP/VP and MCMC runtimes are not so useful, due to differences in the code-base. However, MCMC would have to be very efficient indeed to compete with the VMP, as MCMC must run at each $\psi \in \Psi$ of interest. If the dimension of Ψ is even moderately large then this is impractical. In Section 6.3 we considered a substantial real problem where MCMC on the full data set is too slow to be useful for even a single run. The run time quoted in Table 5 is for a small subset of the data and used the BlackJAX Cabezas et al. (2024) implementation of a NUTS Hoffman et al. (2014) MCMC, so it is at least up to date. The comparison with the VP is more straightforward as the codebase is the same and the run time for fitting the VMP at all ψ and the VP at a single ψ is essentially the same: the extra cost of sampling ψ and forming an empirical estimate of $\overline{\text{ELBO}}$ in (4) is slight.

Table 4 show the architecture and training parameters used to specify and fit our normalising flows. Suitable architectures are relatively simple, as normalising flows are so expressive, we found there is little to be gained from elaboration. This is important when we do VI with the reverse KL. If the flow is expressive then problems with under-dispersed variational approximation are reduced. In this paper we have compared the VMP against MCMC baselines in Figures 1, 2, 14, 9, 10 and 11 where coverage is excellent. In the more challenging example in Section E.3.2 in the Supplement, the coverage in Figure 16 for the key profile-locations is good. Coverage for the zero-inflation parameters ζ in Figure 18 is fair. However the variational posteriors in Figure 17 are under-dispersed. If these were important for the inference then further experimentation with flow architecture would be necessary.

Recent work by [Lipman et al. \(2023\)](#) on flow matching methods for fitting continuous normalising flows to build generative models for complex data distributions show very good expressive power with numerically stable fitting procedures. The corresponding flow matching methods for posterior approximation given in [Wildberger et al. \(2023\)](#) inherit these properties. It is at least conceptually straightforward to extend the amortisation to cover prior hyperparameters and this should deliver greater approximation accuracy. However, the approach is necessarily amortised over data as the flow training needs target samples. It is unclear how these methods might be used to approximate posteriors in GBI and SMI, as there is no generative model for the data in that case, and a solution to this problem would be very useful.

The code to reproduce all the experiments and figures of this paper can be found online at <https://github.com/llaurabatt/amortised-variational-flows.git>.

References

- Ambrogioni, L., Güçlü, U., Berezutskaya, J., van den Borne, E., Güçlütürk, Y., Hinne, M., Maris, E., and van Gerven, M. (2019). “Forward Amortized Inference for Likelihood-Free Variational Marginalization.” In Chaudhuri, K. and Sugiyama, M. (eds.), *Proceedings of the Twenty-Second International Conference on Artificial Intelligence and Statistics*, volume 89 of *Proceedings of Machine Learning Research*, 777–786. PMLR.
URL <https://proceedings.mlr.press/v89/ambrogioni19a.html> 2
- Battaglia, L. and Nicholls, G. (2024). “Supplement of Amortising Variational Bayesian Inference over prior hyperparameters with a Normalising Flow.” DOI: 10.1214/[provided by typesetter]. 12, 19, 20
- Bissiri, P. G., Holmes, C. C., and Walker, S. G. (2016). “A general framework for updating belief distributions.” *Journal of the Royal Statistical Society: Series B (Statistical Methodology)*, 78(5): 1103–1130.
URL <http://doi.wiley.com/10.1111/rssb.12158> 1, 10, 5
- Bitzer, M., Meister, M., and Zimmer, C. (2023). “Amortized Inference for Gaussian Process Hyperparameters of Structured Kernels.”
URL <https://arxiv.org/abs/2306.09819> 3
- Blei, D. M., Kucukelbir, A., and McAuliffe, J. D. (2017). “Variational inference: A review for statisticians.” *Journal of the American statistical Association*, 112(518): 859–877. 4
- Cabezas, A., Corenflos, A., Lao, J., and Louf, R. (2024). “BlackJAX: Composable Bayesian inference in JAX.” 21, 22
- Carmona, C. U., Haines, R. A., Loake, M. A., Benskin, M., and Nicholls, G. K. (2024). “Simultaneous Reconstruction of Spatial Frequency Fields and Sample Locations via Bayesian Semi-Modular Inference.”
URL <https://arxiv.org/abs/2412.05763> 3, 7, 15, 16, 17, 19, 18, 20, 22

- Carmona, C. U. and Nicholls, G. K. (2020). “Semi-Modular Inference: enhanced learning in multi-modular models by tempering the influence of components.” In Silvia, C. and Calandra, R. (eds.), *Proceedings of the 23rd International Conference on Artificial Intelligence and Statistics, AISTATS 2020*, 4226–4235. PMLR. ArXiv: 2003.06804. URL <http://arxiv.org/abs/2003.06804> 3, 8, 9, 10, 14, 5
- (2022). “Scalable Semi-Modular Inference with Variational Meta-Posteriors.” ArXiv: 2204.00296. URL <https://github.com/chriscarmona/modularbayes> 1, 2, 3, 4, 7, 9, 10, 11, 5, 6, 26
- Cooper, A., Simpson, D., Kennedy, L., Forbes, C., and Vehtari, A. (2024). “Cross-Validatory Model Selection for Bayesian Autoregressions with Exogenous Regressors.” *Bayesian Analysis*, 1 – 25. URL <https://doi.org/10.1214/23-BA1409> 9
- Dinh, L., Sohl-Dickstein, J., and Bengio, S. (2016). “Density estimation using Real NVP.” In *Proceedings of the 5th International Conference on Learning Representations, ICLR 2017*. ArXiv: 1605.08803. URL <http://arxiv.org/abs/1605.08803> 2, 1
- Durkan, C., Bekasov, A., Murray, I., and Papamakarios, G. (2019). “Neural Spline Flows.” In *Proceedings of the 33rd Conference on Neural Information Processing Systems, NeurIPS 2019*. ArXiv: 1906.04032. URL <http://arxiv.org/abs/1906.04032> 2, 5, 1, 25
- Elsemüller, L., Olischläger, H., Schmitt, M., Bürkner, P.-C., Koethe, U., and Radev, S. T. (2024). “Sensitivity-Aware Amortized Bayesian Inference.” *Transactions on Machine Learning Research*. URL <https://openreview.net/forum?id=Kxtpa9rvM0> 4
- Fortuin, V. (2022). “Priors in bayesian deep learning: A review.” *International Statistical Review*, 90(3): 563–591. 2
- Frazier, D. T. and Nott, D. J. (2023a). “Accurate semi-modular posterior inference with a user-defined loss function.” URL <https://arxiv.org/abs/2301.10911> 2, 11, 5
- (2023b). “Cutting feedback and modularized analyses in generalized Bayesian inference.” URL <https://arxiv.org/abs/2202.09968> 11, 5
- Gao, R., Deistler, M., and Macke, J. H. (2023). “Generalized Bayesian Inference for Scientific Simulators via Amortized Cost Estimation.” In *Thirty-seventh Conference on Neural Information Processing Systems*. URL <https://openreview.net/forum?id=ZARaiV25CW> 4
- Gelman, A. and Yao, Y. (2020). “Holes in Bayesian statistics.” *Journal of Physics G: Nuclear and Particle Physics*, 48(1): 014002. 2
- Gershman, S. and Goodman, N. (2014). “Amortized inference in probabilistic reasoning.” In *Proceedings of the Annual Meeting of the Cognitive Science Society*, vol-

- ume 36.
URL <https://escholarship.org/uc/item/34j1h7k5> 2
- Giordano, R., Broderick, T., and Jordan, M. I. (2018). “Covariances, robustness, and variational Bayes.” *Journal of Machine Learning Research*, 19: 1–49. ArXiv: 1709.02536.
URL <http://jmlr.org/papers/v19/17-670.html>. 3
- Giordano, R., Liu, R., Jordan, M. I., and Broderick, T. (2022). “Evaluating Sensitivity to the Stick-Breaking Prior in Bayesian Nonparametrics.” *Bayesian Analysis*, -1(-1): 1–67. Publisher: International Society for Bayesian Analysis.
URL <https://projecteuclid.org/journals/bayesian-analysis/advance-publication/Evaluating-Sensitivity-to-the-Stick-Breaking-Prior-in-Bayesian-Nonparametrics/10.1214/22-BA1309.full> 3
- Golinski, A., Wood, F., and Rainforth, T. (2019). “Amortized Monte Carlo Integration.” In Chaudhuri, K. and Salakhutdinov, R. (eds.), *Proceedings of the 36th International Conference on Machine Learning*, volume 97 of *Proceedings of Machine Learning Research*, 2309–2318. PMLR.
URL <https://proceedings.mlr.press/v97/golinski19a.html> 6
- Grünwald, P. and Ommen, T. v. (2017). “Inconsistency of Bayesian Inference for Misspecified Linear Models, and a Proposal for Repairing It.” *Bayesian Analysis*, 12(4): 1069–1103. Publisher: International Society for Bayesian Analysis.
URL <https://projecteuclid.org/journals/bayesian-analysis/volume-12/issue-4/Inconsistency-of-Bayesian-Inference-for-Misspecified-Linear-Models-and-a/10.1214/17-BA1085.full> 1, 2, 3, 10
- Haines, R. A. (2016). “Simultaneous Reconstruction of Spatial Frequency Fields and Field Sample Locations.” PhD thesis, University of Oxford.
URL <http://arxiv.org/abs/1708.08719> 16, 17
- Hoffman, M. D., Gelman, A., et al. (2014). “The No-U-Turn sampler: adaptively setting path lengths in Hamiltonian Monte Carlo.” *J. Mach. Learn. Res.*, 15(1): 1593–1623. 21, 22
- Holmes, C. C. and Walker, S. G. (2017). “Assigning a value to a power likelihood in a general Bayesian model.” *Biometrika*, 104(2): 497–503. 3
- Huang, C.-W., Krueger, D., Lacoste, A., and Courville, A. (2018). “Neural Autoregressive Flows.” In Dy, J. and Krause, A. (eds.), *Proceedings of the 35th International Conference on Machine Learning*, volume 80 of *Proceedings of Machine Learning Research*, 2078–2087. PMLR.
URL <https://proceedings.mlr.press/v80/huang18d.html> 2, 5, 6, 7, 1, 3
- Jaini, P., Selby, K. A., and Yu, Y. (2019). “Sum-of-squares polynomial flow.” In *International Conference on Machine Learning*, 3009–3018. PMLR. 5, 1
- Jewson, J. and Rossell, D. (2022). “General Bayesian loss function selection and the use of improper models.” *Journal of the Royal Statistical Society Series B: Statistical Methodology*, 84(5): 1640–1665. 10

- Jewson, J., Smith, J. Q., and Holmes, C. (2024). “On the Stability of General Bayesian Inference.”
URL <https://arxiv.org/abs/2301.13701> 10
- Jordan, M. I., Ghahramani, Z., Jaakkola, T. S., and Saul, L. K. (1999). “An introduction to variational methods for graphical models.” *Machine learning*, 37: 183–233. 4
- Kingma, D. P. and Welling, M. (2013). “Auto-encoding variational bayes.” *arXiv preprint arXiv:1312.6114*. 2, 3
- Lipman, Y., Chen, R. T. Q., Ben-Hamu, H., Nickel, M., and Le, M. (2023). “Flow Matching for Generative Modeling.” In *The Eleventh International Conference on Learning Representations*.
URL <https://openreview.net/forum?id=PqvMRDCJT9t> 22
- Liu, S., Sun, X., Ramadge, P. J., and Adams, R. P. (2020). “Task-agnostic amortized inference of gaussian process hyperparameters.” *Advances in Neural Information Processing Systems*, 33: 21440–21452. 3
- Lunn, D., Best, N., Spiegelhalter, D., Graham, G., and Neuenschwander, B. (2009). “Combining MCMC with ‘sequential’PKPD modelling.” *Journal of Pharmacokinetics and Pharmacodynamics*, 36: 19–38. 11, 5
- Lyddon, S. P., Holmes, C., and Walker, S. (2019). “General Bayesian updating and the loss-likelihood bootstrap.” *Biometrika*, 106(2): 465–478. 3
- Margossian, C. C. and Blei, D. M. (2023). “Amortized Variational Inference: When and Why?” 2, 6
- Maucort-Boulch, D., Franceschi, S., Plummer, M., and Group, I. H. P. S. S. (2008). “International correlation between human papillomavirus prevalence and cervical cancer incidence.” *Cancer Epidemiology Biomarkers & Prevention*, 17(3): 717–720. 13
- McIntosh, A., Samuels, M. L., Benskin, M., Laing, M., and Williamson, K. (1986). *A linguistic atlas of late mediaeval English*. Aberdeen University Press. 15, 17
- McLatchie, Y., Fong, E., Frazier, D. T., and Knoblauch, J. (2024). “Predictive performance of power posteriors.”
URL <https://arxiv.org/abs/2408.08806> 8, 9
- Meng, X.-L. (1994). “Multiple-Imputation Inferences with Uncongenial Sources of Input.” *Statistical Science*, 9(4): 538 – 558.
URL <https://doi.org/10.1214/ss/1177010269> 11, 5
- Papamakarios, G., Nalisnick, E., Rezende, D. J., Mohamed, S., and Lakshminarayanan, B. (2021). “Normalizing Flows for Probabilistic Modeling and Inference.” *J. Mach. Learn. Res.*, 22(1). 2, 5, 6, 7, 1, 3
- Plummer, M. (2015). “Cuts in Bayesian graphical models.” *Statistics and Computing*, 25(1): 37–43.
URL <http://link.springer.com/10.1007/s11222-014-9503-z> 11, 13, 5

- Rezende, D. and Mohamed, S. (2015). “Variational inference with normalizing flows.” In *International conference on machine learning*, 1530–1538. PMLR. 2, 8, 1
- Robbins, H. (1956). “An Empirical Bayes Approach to Statistics.” In *Proceedings of the Third Berkeley Symposium on Mathematical Statistics and Probability, 1954–1955, Vol. I*, 157–163. Berkeley/Los Angeles: Univ. of California Press. 2
- Syring, N. and Martin, R. (2019). “Calibrating general posterior credible regions.” *Biometrika*, 106(2): 479–486. 3
- Vehtari, A., Gelman, A., and Gabry, J. (2017). “Practical Bayesian model evaluation using leave-one-out cross-validation and WAIC.” *Statistics and Computing*, 27(5): 1413–1432. ArXiv: 1507.04544 Publisher: Springer US ISBN: 1507.04544. URL <http://link.springer.com/10.1007/s11222-016-9696-4> 3, 8
- Wainwright, M. J., Jordan, M. I., et al. (2008). “Graphical models, exponential families, and variational inference.” *Foundations and Trends® in Machine Learning*, 1(1–2): 1–305. 4
- Warwick, J. and Jones, M. C. (2005). “Choosing a robustness tuning parameter.” *Journal of Statistical Computation and Simulation*, 75(7): 581–588. URL <https://doi.org/10.1080/00949650412331299120> 10
- Watanabe, S. (2010). “Asymptotic equivalence of Bayes cross validation and widely applicable information criterion in singular learning theory.” *Journal of machine learning research*, 11(12). 3, 8
- Wildberger, J. B., Dax, M., Buchholz, S., Green, S. R., Macke, J. H., and Schölkopf, B. (2023). “Flow Matching for Scalable Simulation-Based Inference.” In *Thirty-seventh Conference on Neural Information Processing Systems*. URL <https://openreview.net/forum?id=D2cS6SoY1P> 22
- Winter, S., Melikechi, O., and Dunson, D. B. (2023). “Sequential Gibbs Posteriors with Applications to Principal Component Analysis.” *arXiv preprint arXiv:2310.12882*. 3, 10
- Wu, M., Choi, K., Goodman, N., and Ermon, S. (2020). “Meta-Amortized Variational Inference and Learning.” *Proceedings of the AAAI Conference on Artificial Intelligence*, 34(04): 6404–6412. URL <https://ojs.aaai.org/index.php/AAAI/article/view/6111> 3, 6
- Wu, P.-S. and Martin, R. (2023). “A Comparison of Learning Rate Selection Methods in Generalized Bayesian Inference.” *Bayesian Analysis*, 18(1): 105 – 132. URL <https://doi.org/10.1214/21-BA1302> 3, 10
- Yu, X., Nott, D. J., and Smith, M. S. (2023). “Variational Inference for Cutting Feedback in Misspecified Models.” *Statistical Science*, 38(3): 490 – 509. URL <https://doi.org/10.1214/23-STS886> 11

Acknowledgments

The authors thank Chris Carmona and Michael Benskin for valuable insight and advice. We also thank the Google TPU Research Cloud (TRC) program for supporting the project.

Funding

LB was supported by a Clarendon Scholarship from the University of Oxford. The compute was provided by Google through the TPU Research Cloud (TRC) program.

Supplementary Material

Appendix A: Variational Bayes with Normalising Flows

In this section we give the VI setup for a normalising flow without amortising. This includes some calculation details which carry over straightforwardly to the amortised setting.

We work with families of densities defined by “normalising flows” exploiting specific features of the flow structure for our purpose. Normalising flows were invented by Tabak and Vanden-Eijnden (2010) and Tabak and Turner (2013). The framework gained popularity through the works of Dinh et al. (2016) in density estimation and Rezende and Mohamed (2015) in VI. Subsequently, normalising flows and autoregressive models have been successfully combined in Masked Autoregressive Flows (Papamakarios et al., 2017), Inverse Autoregressive Flows (Kingma et al., 2016) and the unifying framework of Neural Autoregressive Flows (Huang et al., 2018). NFs are also used in the context of VAEs to achieve flexible priors/posteriors (Kingma and Dhariwal (2018), Chen et al. (2016), Morrow and Chiu (2020), Zhang et al. (2024)). See Papamakarios et al. (2021) for an introduction and overview.

A.1 Auto-regressive normalising flow

A normalising flow with parameters $\lambda \in \Lambda$ is a transformation $T(\cdot; \lambda) : \mathbb{R}^p \rightarrow \mathbb{R}^p$ which is invertible and continuously differentiable in \mathbb{R}^p . Let $q(\epsilon)$, $\epsilon \in \mathbb{R}^p$ be some simple distribution, for example, $\epsilon \sim N(0_p, I_p)$. If we set $\theta = T(\epsilon; \lambda)$ then

$$q(\theta; \lambda) = q(\epsilon) |\det(J_T(\epsilon; \lambda))|^{-1} \Big|_{\epsilon=T^{-1}(\theta; \lambda)},$$

with Jacobian

$$J_T(\epsilon; \lambda) = \frac{\partial T(\epsilon; \lambda)}{\partial \epsilon^T}.$$

We parameterise $T(\epsilon; \lambda)$ using an auto-regressive transformer-conditioner structure (as described in e.g., Huang et al. (2018), Jaini et al. (2019)). For $\epsilon \in \mathbb{R}^p$ let $\epsilon_{<i} = (\epsilon_1, \dots, \epsilon_{i-1})$. A transformer $\tau(\epsilon_i; h_i) \in R$ is a strictly monotone function of $\epsilon_i \in R$ with fixed parameters $h_i \in \mathbb{R}^{d_h}$ (for example, Durkan et al. (2019) takes τ to be a spline). A conditioner $c_i : \mathbb{R}^{i-1} \rightarrow \mathbb{R}^{d_h}$ is a map which returns a set of set of parameters for the transformer via $h_i = c_i(\epsilon_{<i}; \lambda_i)$. The conditioners do not need to be invertible. If we take

$$\begin{aligned} \theta_1 &= \tau(\epsilon_1, h_1), & h_1 &= c_1(\lambda_1) \\ \theta_2 &= \tau(\epsilon_2, h_2), & h_2 &= c_2(\epsilon_{<2}; \lambda_2) \\ \theta_3 &= \tau(\epsilon_3, h_3), & h_3 &= c_3(\epsilon_{<3}; \lambda_3) \\ & \vdots & & \end{aligned}$$

$$\theta_p = \tau(\epsilon_p, h_p), \quad h_p = c_p(\epsilon_{<p}; \lambda_p)$$

then this defines $\theta = T(\epsilon; \lambda)$ with $\partial\theta_i/\partial\epsilon_j = 0$ for $j > i$ so that

$$\det(J_T(\epsilon; \lambda)) = \prod_{i=1}^p \frac{\partial\tau(\epsilon_i; h_i)}{\partial\epsilon_i}.$$

Given λ, ψ and θ we can recover ϵ as $(\lambda_1, \psi) \rightarrow h_1 \rightarrow \epsilon_1$ as τ is invertable at fixed h_1 and then by induction, $(\epsilon_{<i}, \lambda_i) \rightarrow h_i \rightarrow \epsilon_i$. Let $\epsilon(\theta) = T^{-1}(\theta; \lambda)$. If we fix $\lambda = (\lambda_1, \dots, \lambda_p)$ then we have a parameterised map determining the family of variational densities $q(\cdot; \lambda)$, $\lambda \in \Lambda$ we can represent at each $\psi \in \Psi$.

Having parameterised the variational family we seek the optimal approximating density $q(\theta; \lambda_\psi^*)$ minimising the reverse-KL divergence, taking

$$\lambda^* = \arg \min_{\lambda} D_{KL}(q(\theta; \lambda) || p(\theta|Y, \psi)), \quad (29)$$

where

$$D_{KL}(q(\theta; \lambda) || p(\theta|Y, \psi)) = E_{\theta \sim q(\theta; \lambda)} \left[\log \frac{q(\theta; \lambda)}{p(\theta|Y, \psi)} \right]. \quad (30)$$

If the variational family is sufficiently expressive then $\pi(\theta|Y, \psi) \simeq q(\theta; \lambda^*, \psi)$. This approach has the disadvantage that, the optimal fit is often underdispersed. The approximation is improved by using an expressive variational family such as a normalising flow.

We minimise (30) at fixed ψ by maximising the evidence lower bound (ELBO) in (1). We write $\text{ELBO}(\lambda|\psi)$ to emphasise this is the ELBO for a variational approximation $q(\theta; \lambda)$ at a fixed ψ -value only, and λ_ψ^* to emphasise the ψ -dependence of λ^* when we don't amortise. We call $q(\theta; \lambda_\psi^*)$ the (usual) variational posterior (VP). It must be fitted separately at each ψ of interest.

The NF setup allows for reparametrising the ELBO in terms of the fixed and much simpler distribution $q(\epsilon)$ (*reparametrisation trick*). The ELBO objective can be written

$$\begin{aligned} \text{ELBO}(\lambda|\psi) &= E_{\epsilon \sim q(\epsilon)} [\log p(T(\epsilon; \lambda), Y|\psi) - \log q(\epsilon) + \log |\det J_T(\epsilon; \lambda)|] \\ &\propto E_{\epsilon \sim q(\epsilon)} [\log p(T(\epsilon; \lambda), Y|\psi) + \log |\det J_T(\epsilon; \lambda)|] \end{aligned} \quad (31)$$

and for any given λ can be estimated by Monte Carlo, using samples from the base distribution $q(\epsilon)$.

A.2 Auto-regressive flow as a universal approximator

In this section we give the universal approximator result of [Huang et al. \(2018\)](#).

We can compose the autoregressive maps $T(\cdot; \lambda)$ taking the components of θ in different orders to get more expressive maps. This is done for efficiency. In fact, for

common choices of τ and c_i , $i = 1, \dots, p$, a single autoregressive flow is a universal approximator (Huang et al., 2018), meaning we can approximate any fixed target density $p(\theta|Y, \psi)$ with arbitrary precision by taking increasingly general transformer and conditioner functions. We quote this result here.

Huang et al. (2018) defines a class of flows called Deep Sigmoidal Flows and shows that they universally approximate continuous densities with bounded domain. Huang et al. (2018) give a more general result but for our purposes the following is sufficient.

Lemma A.1. (Theorem 1 of Huang et al. (2018)) *Let θ be a p -dimensional continuous random variable with a probability density $p(\cdot|Y, \psi)$ which is continuous and strictly positive on a bounded rectangular region of \mathbb{R}^p and let \mathcal{P} be the corresponding class of distributions. The family of Autoregressive Deep Sigmoidal Flows is a universal approximator for distributions in \mathcal{P} in the sense of Definition 3.1.*

All this is at fixed $\psi \in \Psi$. As ψ varies λ must change to match $q(\theta; \lambda)$ and $p(\theta|Y, \psi)$. We extend it to the amortised case where we write $q(\theta; \lambda, \psi)$ below. In that setting $q(\theta; \lambda, \psi)$ approximates $p(\theta|Y, \psi)$ at each $\psi \in \Psi$ without varying λ . We will see that an autoregressive flow which is a universal approximator for fixed ψ can be modified to give a universal approximator in the amortised setting.

In practice, conditioners are often implemented as *masking conditioners*: i.e., neural networks (typically, MLPs) where the weight matrices of each layer are multiplied by binary matrices that mask connections and guarantee autoregressive features while retaining the efficiency of the original network. Masked autoregressive flows are efficient to evaluate, as at each step k the parameters (h_1, \dots, h_p) can be obtained in parallel in one neural network pass, but not as efficient to invert. In our application, we use even simpler *coupling layers*, that are equally fast to evaluate or invert. Such a conditioner is a multi-layered network where layer k partitions its input $\epsilon^{(k-1)}$ into two sub-vectors, and obtains $\epsilon^{(k)}$ by keeping the first sub-vector fixed and transforming the second sub-vector with e.g., a neural network having the first sub-vector as input. As Papamakarios et al. (2021) point out, a single coupling-layer conditioner cannot be a universal approximator. They can be stacked to reproduce a general autoregressive flow. However, that would remove the advantage they offer, which is to trade off expressive power for computational efficiency.

Appendix B: Proof of Theorem 3.2

Theorem 3.2. *Let $\omega = (\psi, \theta)$ be a $d = d_\psi + p$ -dimensional continuous random variable with a probability density $\pi(\omega) = \rho(\psi)p(\theta|Y, \psi)$ which is continuous and strictly positive on a bounded rectangular region $\Omega = \Psi \times \Theta$ of $\mathbb{R}^{-d_\psi+p}$ and let $(\mathbb{T}, \mathbb{C}, \mathbb{L})$ be a class of autoregressive flows satisfying Definition 3.1. There exists a sequence of flows $(\tau^{(k)}, c^{(k)}, \lambda^{(k)})$ (not depending on ψ) such that for all $(\psi, \theta_{<i}) \in \Psi \times \Theta_{<i}$ the transformed random variables*

$$\theta_i^{(k)} = \tau^{(k)}(\epsilon_i, c_i^{(k)}(\epsilon_{<i}(\theta_{<i}, \psi), \psi; \lambda_i^{(k)})), \quad i = 1, \dots, p,$$

satisfy $\theta_i^{(k)} \xrightarrow{D} p(\cdot|Y, \theta_{<i}, \psi)$ as $k \rightarrow \infty$ (where $\epsilon_{<i}(\theta_{<i}, \psi)$ is given by inversion of (2)).

Proof. Index the entries in $\omega \in \Psi \times \Theta$ from $i = -d_\psi + 1$ to $i = p$. Since $(\mathbb{T}, \mathbb{C}, \mathbb{L})$ universally approximates distributions in \mathcal{D} , and this includes $\pi(\omega) = \rho(\psi)p(\theta|Y, \psi)$, there exists a sequence $(\tau^{(k)}, c^{(k)}, \lambda^{(k)})$ $k \geq 1$ such that $\omega_i^{(k)} \xrightarrow{D} \pi(\cdot|\omega_{<i})$ for each $\omega_{<i} \in \Omega_{<i}$ (see Definition 3.1). This sequence doesn't depend on ψ by construction (as ψ is now an input to the flow like ϵ).

Suppose the base density is $q(\psi, \epsilon) = \rho(\psi)q(\epsilon)$ so the variables input to the flow are $\psi_1, \dots, \psi_{d_\psi}, \epsilon_1, \dots, \epsilon_p$ in that order. The map from ψ, ϵ to ω begins with d_ψ conditioner-transformer steps which transform ψ to new variables $\omega_{-d_\psi+1}, \dots, \omega_0$ say.

$$\begin{aligned} \omega_{-d_\psi+1}^{(k)} &= \tau_{-d_\psi+1}^{(k)}(\psi_1; h_{-d_\psi+1}^{(k)}) & h_{-d_\psi+1}^{(k)} &= c_{-d_\psi+1}^{(k)}(\lambda_{-d_\psi+1}^{(k)}) \\ &\vdots & &\vdots \\ \omega_0^{(k)} &= \tau_0^{(k)}(\psi_{<d_\psi}; h_0^{(k)}) & h_0^{(k)} &= c_0^{(k)}(\psi_{<d_\psi}; \lambda_0^{(k)}) \end{aligned}$$

The remainder of the layers in the autoregression are the same as in (2).

$$\begin{aligned} \omega_1^{(k)} &= \tau_1^{(k)}(\epsilon_1; h_1^{(k)}) & h_1^{(k)} &= c_1^{(k)}(\psi; \lambda_1^{(k)}) \\ \omega_2^{(k)} &= \tau_2^{(k)}(\epsilon_2; h_2^{(k)}) & h_2^{(k)} &= c_2^{(k)}(\epsilon_1, \psi; \lambda_2^{(k)}) \\ &\vdots & &\vdots \\ \omega_i^{(k)} &= \tau_i^{(k)}(\epsilon_i; h_i^{(k)}) & h_i^{(k)} &= c_i^{(k)}(\epsilon_{<i}, \psi; \lambda_i^{(k)}) \\ &\vdots & &\vdots \\ \omega_p^{(k)} &= \tau_p^{(k)}(\epsilon_p; h_p^{(k)}) & h_p^{(k)} &= c_p^{(k)}(\epsilon_{<p}, \psi; \lambda_p^{(k)}) \end{aligned}$$

Fix some $\psi \in \Psi$ and consider what happens in the second half of the flow as i runs from 1 to p . If $i = 1$ and we take some $\theta_1 \in \Theta_1$ and set $\omega_1^{(k)} = \theta_1$ then $\theta_1 = \tau(\epsilon_1; h_1^{(k)})$ has a unique solution for ϵ_1 as $h_1^{(k)}$ is fixed by ψ . If $i > 1$ and we fix $\theta_{<i} \in \Theta_{<i}$ and set $\omega_j^{(k)} = \theta_j$ for each $j = 1, \dots, i-1$ then $\epsilon_1(\psi, \theta_1), \dots, \epsilon_{i-1}(\psi, \theta_{<i})$ can be obtained by inversion starting from ϵ_1 . For $i > 0$, $\pi(\omega_i|\omega_{<i}) = p(\theta_i|Y, \theta_{<i}, \psi)$ so if for any $i > 0$ and $(\psi, \Theta_{<i}) \in \Psi \times \Theta_{<i}$ we set

$$\omega_i^{(k)} = \tau_i^{(k)}(\epsilon_i; c_i^{(k)}(\epsilon_{<i}, \psi; \lambda_i^{(k)}))$$

with $\epsilon_{<i}$ determined by inversion from $\theta_{<i}$ and ψ then $\omega_i^{(k)} \xrightarrow{D} p(\cdot|Y, \theta_{<i}, \psi)$ as $k \rightarrow \infty$.

When we come to fit an amortised variational approximation we do not need to include layers $j = -d_\psi, \dots, 0$ as all that matters for the proof is that Ψ is bounded and ψ is passed as input into the conditioners in layers $j = 1, \dots, p$. \square

Appendix C: Background on SMI with the VMP

In this section we add some further background on the SMI and VMP methods set out in Sections 5.1 and 5.2.

When we fit models with extrinsic parameters shared across data-models, it is common to have conflict between modules: if we analyse the data sets separately then for any given extrinsic parameter we get one posterior distribution for each module it belongs to; if the modules are “uncongenial” (Meng, 1994) then these distributions may express conflicting beliefs about the parameter. A formal definition of a module is given in Liu and Goudie (2022b).

SMI assumes well-specified and mis-specified modules have been identified and tempers the influence of bad modules on the parameters shared between good and bad modules. Different ways of parameterising the tempering are given in Carmona and Nicholls (2020); Nicholls et al. (2022); Chakraborty et al. (2022) and Frazier and Nott (2023a). These SMI belief-updates are coherent and valid (Carmona and Nicholls, 2020; Nicholls et al., 2022) in the sense of Bissiri et al. (2016). In Section 5.2 we use the framework given in Carmona and Nicholls (2020).

When $\eta = 0$ in SMI the belief update is called the “cut-posterior” in Lunn et al. (2009) and Plummer (2015). This is natural and was anticipated in Liu et al. (2009) and several earlier applied data analyses. Cut models are studied in Jacob et al. (2017) and Pompe and Jacob (2021), Liu and Goudie (2022a) and Yu et al. (2023) and SMI and Cut models in Frazier and Nott (2023b), and Frazier and Nott (2023a).

MCMC targeting the SMI posterior in (20) is not straightforward as $p(\theta|\delta, Y; \psi)$ has a marginal factor $p(Y|\delta; \psi)$ in the denominator (which cancels out in (19)). However, a form of nested MCMC can be used, targeting $p_{pow}(\delta, \tilde{\theta}|Y, Z; \tilde{\psi})$ and sampling $p(\theta|\delta, Y; \psi)$ for each sampled δ . Carmona and Nicholls (2020) explain why this seemingly inefficient scheme is often quite practical, though it does suffer from “double asymptotics” and has the usual strengths and weaknesses of MCMC. While variants of MCMC have been proposed to address these issues for SMI-posteriors and cut-posteriors (Plummer, 2015; Jacob et al., 2020; Liu and Goudie, 2022b), better guarantees in terms of sample quality have often come at the expense of speed and scalability. We use a form of nested MCMC (Plummer, 2015) as ground truth in small problems, for comparison purposes.

When we come to fit the variational approximation in (22) we seek a set of variational parameters λ^* maximising a utility that rewards for the variational approximation being close to the SMI-posterior at any value of the hyperparameters $\tilde{\psi}$. Following Carmona and Nicholls (2022), this must be done in two stages in order to stop the variational approximation from introducing uncontrolled information flow between modules. We first set λ_1^*, λ_3^* to minimise the expectation over the KL divergence to the power-posterior

$$\lambda_1^*, \lambda_3^* = \underset{(\lambda_1, \lambda_3)}{\operatorname{argmin}} \mathbb{E}_{\tilde{\psi} \sim \rho} [D_{KL}(q_1(\delta; \lambda_1, \tilde{\psi})q_3(\tilde{\theta}|\delta; \lambda_3, \tilde{\psi})||p_{pow}(\delta, \tilde{\theta}|Y, Z; \tilde{\psi})))] \quad (32)$$

and then choose λ_2^* to minimise the KL divergence to the part of the posterior constituting the analysis stage

$$\lambda_2^* = \underset{\lambda_2}{\operatorname{argmin}} \mathbb{E}_{\tilde{\psi} \sim \rho} [D_{KL}(q_1(\delta; \lambda_1^*, \tilde{\psi})q_2(\theta|\delta; \lambda_2, \tilde{\psi})||p(\theta|Y, \delta; \psi))] \quad (33)$$

These can be expanded to give the usual ELBO format maximisation target, using the reparameterisation trick and automatic differentiation, as in (31).

As [Carmona and Nicholls \(2022\)](#) show, this setup gives a variational approximation in which information from Y into δ is completely removed at $\eta = 0$, which exactly matches standard variational Bayes using $q_1(\delta; \lambda_1, \psi)q_2(\theta; \delta; \lambda_2, \psi)$ to target $p(\delta, \theta|Y; \psi)$ at $\eta = 1$ and which approximates SMI at all η in the sense that $q(\theta, \tilde{\theta}, \delta; \lambda, \tilde{\psi}) \rightarrow p_{smi}(\phi, \theta, \tilde{\theta}|Y, Z; \tilde{\psi})$ in the limit that the variational family encompasses p_{smi} . Each of the two optimisation stages has the same format as the variational problem in (3) and the discussion of its properties as a universal approximator in Section 3.3 carries over. As noted in that section, we make a small improvement on [Carmona and Nicholls \(2022\)](#) by allowing $\tilde{\psi}$ and ϵ to interact in the conditioner, rather than taking an additive conditioner. The two-stage optimisation process set out above can be implemented in a single step by making use of the stop-gradient operator. We refer the reader to [Carmona and Nicholls \(2022\)](#) for further detail.

Appendix D: Hyperparameter selection for SMI

Setting an objective for hyperparameter selection in SMI, as opposed to regular Bayes, follows the same logic laid out in Section 4, with the main difference being that the marginal likelihood (or ELBO) is no longer a suitable utility, as we are using SMI to treat misspecification. If the objective is prediction, we use the ELPD to select the combined model hyperparameters and learning rate, $\tilde{\psi} = (\psi, \eta)$. As noted in Section 4, when we have two datasets we must select one or both as the target for prediction. If the target is Y then the LOOCV estimator for the (negative) ELPD is

$$\hat{\mathcal{L}}_Y(\tilde{\psi}) = - \sum_{i=1}^n \log(\overline{p(Y_i|Y_{-i}, Z; \tilde{\psi})})$$

where Y_{-i} is the data with the i 'th sample removed and

$$\overline{p(Y_i|Y_{-i}, Z; \tilde{\psi})} = \mathbb{E}_{\delta \sim q_1(\cdot; \lambda_1^*, \tilde{\psi}), \theta \sim q_2(\cdot; \delta, \lambda_2^*, \tilde{\psi})} (p(Y_i|\theta, \delta)).$$

We optimise over parameters of the model and inference taking $(\psi^*, \eta^*) = \tilde{\psi}^*$ with

$$\tilde{\psi}^* = \underset{\tilde{\psi}}{\operatorname{argmin}} \hat{\mathcal{L}}_Y(\tilde{\psi})$$

The final belief update is $p(\delta, \theta|Y, Z; \tilde{\psi}^*) \simeq q_1(\delta; \lambda_1^*, \tilde{\psi}^*)q_2(\theta; \delta, \lambda_2^*, \tilde{\psi}^*)$. The loss $\hat{\mathcal{L}}_Z(\tilde{\psi})$ when the target is Z is defined in a similar way.

When the goal of the inference is parameter estimation and we have a perfectly observed subset of parameters in the same class as the missing values then we target the PMSE. In order to connect to the notation of Section 4 we put the labeled data in the Z -module and the unlabeled data in the Y -module so we identify Y_A in Section 4 with Z in Section 5.1 and Y_M with Y . The posterior in (13) factorises as

$$p(\alpha, X_M|y_P, x_A; \psi) = p(X_M|\alpha, y_M; \psi)p(\alpha|y_A, y_M, x_A; \psi)$$

This matches the factorised Bayes posterior in (19) with the identification $\alpha \rightarrow \delta$ and $X_M \rightarrow \theta$ giving the same setup as in (15), so the VMP setup for SMI carries over. The

duplicated auxiliary variable $\tilde{\theta}$ is a second copy of X_M needed to define the likelihood for Y_M in the power posterior. The power posterior version of (13) is

$$p_{pow}(\alpha, \tilde{X}_M | y_{\mathcal{P}}, x_A; \tilde{\psi}) \propto p(\alpha; \psi) \prod_{m \in M} p(y_m | \alpha, \tilde{X}_m; \psi)^n p(\tilde{X}_m; \psi) \prod_{a \in A} p(y_a | \alpha, x_a; \psi) p(x_a; \psi)$$

and the analysis-posterior is $p(X_M | \alpha, y_M; \psi)$. The variational approximation to the marginal SMI posterior for α, X_M (integrating \tilde{X}_M) is $q_1(\alpha; \lambda_1, \tilde{\psi}) q_2(X_M; \alpha, \lambda_2, \tilde{\psi})$. For the loss estimated using a held out sample $B \subset A$ of the labeled data, the held out samples are added to the unlabeled data. The SMI posterior is

$$p_{smi}(\alpha, \tilde{X}_M, \tilde{X}_B, X_M, X_B | Y_A, Y_M, x_{A \setminus B}; \tilde{\psi}) = p_{pow}(\alpha, \tilde{X}_M, \tilde{X}_B | Y_A, Y_M, x_{A \setminus B}; \tilde{\psi}) \\ \times p(X_M, X_B | Y_M, Y_B; \tilde{\psi}).$$

In this held-out setting we recover the SMI notation with $X_{A \setminus B} \rightarrow Z$, $(Y_M, Y_B) \rightarrow Y$, $\alpha \rightarrow \delta$ and $(X_M, X_B) \rightarrow \theta$. The SMI posterior is approximated with a VMP $q_1(\alpha; \lambda_1, \tilde{\psi}) q_2(X_M, X_B; \alpha, \lambda_2, \tilde{\psi})$ for α, X_M and X_B and we estimate the PMSE with

$$\widehat{\text{PMSE}}_{LMO}(\tilde{\psi}) = \frac{1}{|B|} \sum_{a \in B} \mathbb{E}_{\alpha \sim q_1, X_a \sim q_2} (\|x_a - X_a\|^2 | y_{\mathcal{P}}, x_{A \setminus B}; \tilde{\psi}).$$

Finally $\psi^* = \text{argmin}_{\tilde{\psi}} \widehat{\text{PMSE}}_{LMO}(\tilde{\psi})$. Optimisation is carried out using automatic differentiation with respect to the conditioner inputs to the flow.

Appendix E: Additional experimental results

E.1 Synthetic data

E.1.1 Additional information on the synthetic small dataset experiment

Figure 5 gives a graphical illustration for the data and data generating process of the small synthetic dataset. Figure 6 shows the ELBO and the traces for the four hyperparameters. We can see that they converge to reasonable values, which we have seen to induce sensible posterior approximations in Figure 1.

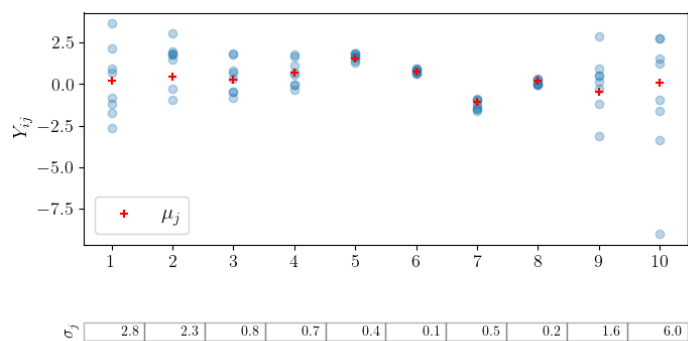


Figure 5: Synthetic data. Data generating process for dataset with $I = 8$ and $J = 10$.

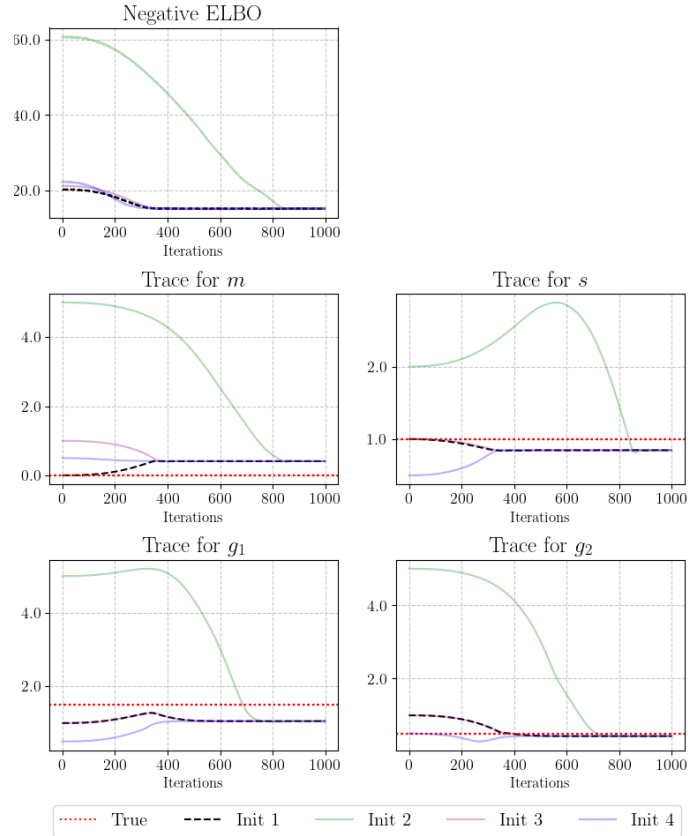


Figure 6: Synthetic data. Training loss and trace plots for hyperparameter optimisation on smaller dataset at different initial values. The run achieving the lowest average loss over the last 20 iterations is highlighted in black. Hyperparameters were selected as the average values over the 20 last iterations corresponding to the highlighted loss.

E.1.2 Additional information on the synthetic large dataset experiment

Figure 7 gives a graphical illustration for the data and data generating process of the large synthetic dataset. Figure 8 shows the ELBO and the traces for the four hyperparameters. It is evident that they converge closely to the true values. The estimated posterior approximations are nearly indistinguishable from MCMC-derived posteriors (see Figures 9 and 10).

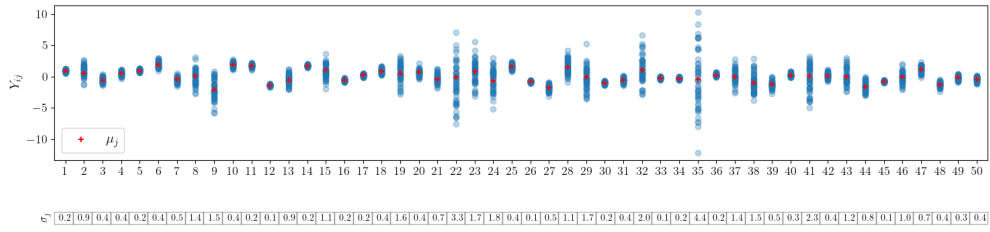


Figure 7: Synthetic data. Data generating process for larger dataset with $I = 50$ and $J = 50$.

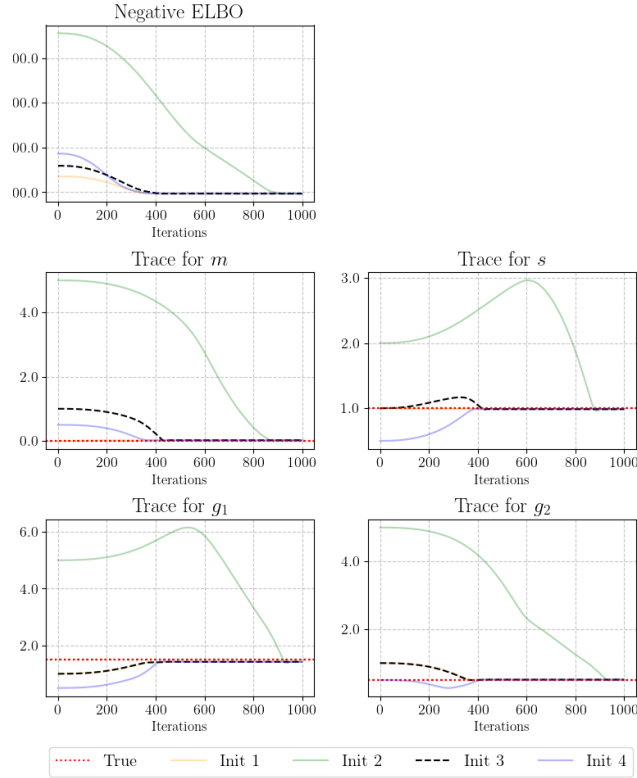


Figure 8: Synthetic data. Training loss and trace plots for hyperparameter optimisation on larger dataset at different initial values. The run achieving the lowest average loss over the last 20 iterations is highlighted in black. Hyperparameters were selected as the average values over the 20 last iterations corresponding to the highlighted loss.

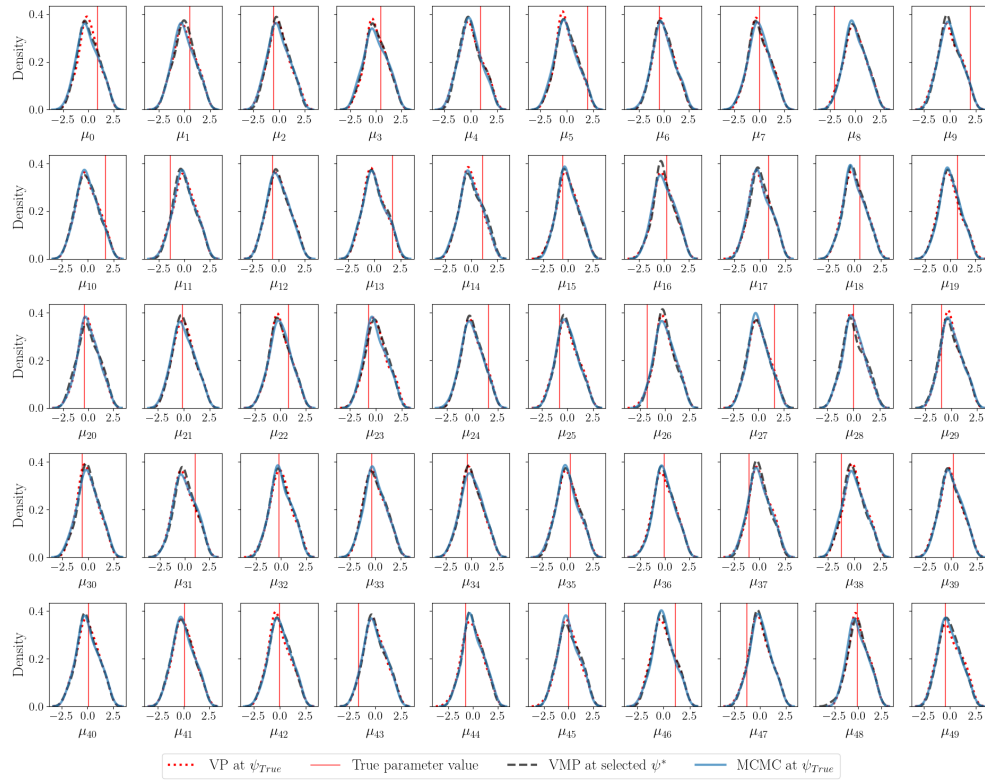


Figure 9: Synthetic larger dataset. Ground truth μ_j posteriors compared to estimated μ_j posteriors at selected hyperparameters.

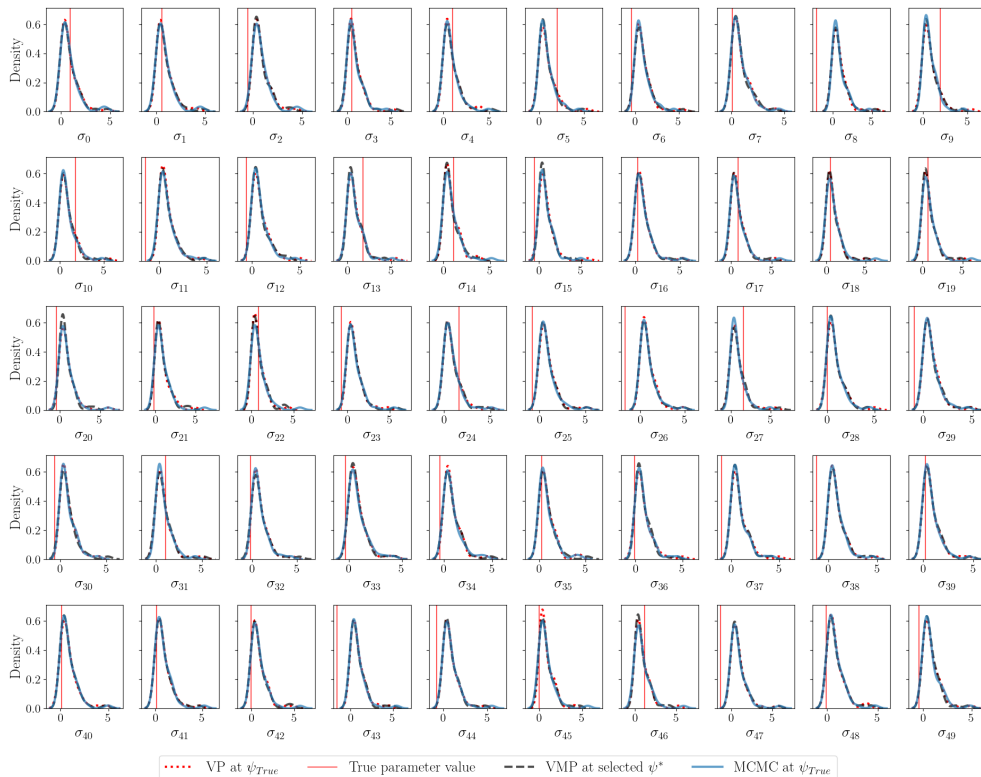


Figure 10: Synthetic larger dataset. Ground truth σ_j posteriors compared to estimated σ_j posteriors at selected hyperparameters.

E.2 HPV data

E.2.1 Tuning hyperparameters in a Bayesian setting

In this section we ignore misspecification in the HPV model and study the problem in a standard Bayes set-up.

We fit the VMP $q(\theta, \delta; \lambda^*, \psi)$ approximation to the HPV posterior $p(\theta, \delta|Y, Z)$ for the HPV data and use the VMP to explore sensitivity to different hyperparameter choices. At each set of values we also run MCMC targeting the posterior at different ψ values, and find good agreement with the VMP sampled at those values, both visually and in terms of Wasserstein distance. As a representative example, Figure 11 shows θ samples from the VMP overlaid with KDE contours for MCMC samples at (a) $\psi = \{1.71, 15\}$ and (b) $\psi = \{11.82, 15\}$ (these were the optimal values depending on whether we target Z or Y prediction, see below). We see good alignment between MCMC and the VMP posterior approximations. There is also hyperparameter dependence (compare Figures 11a and 11b). The VMP captures this well, without the need for MCMC.

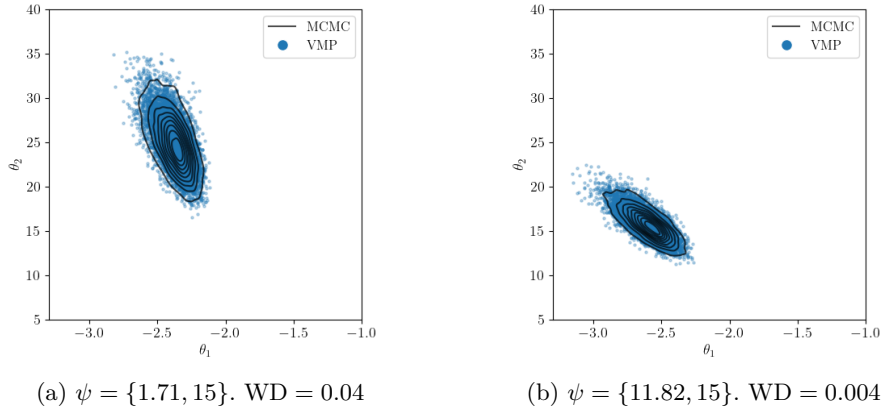


Figure 11: Epidemiological data in Bayes setting. VMP samples overlaid with KDE contour plots of MCMC samples, at different values of hyperparameters $\psi = \{c_1, c_2\}$. The Wasserstein Distance (WD) between the two distributions is given below each plot.

The data set is small so it is computationally feasible to estimate ψ^* by optimising the LOOCV ELPD-estimator $\hat{\mathcal{L}}(\psi)$ in (11) over ψ using Stochastic Gradient Descent (SGD), taking derivatives over ψ via automatic differentiation. We do this for both Z and Y prediction. In practical situations, the decision regarding which module to target rests with the researcher. Figure 12 shows the loss and corresponding optimisation traces for different initial ψ values. We select as optimal ψ^* the values achieving the lowest loss over all initialisations. The ELPD varies significantly as the hyperparameters change. Good values of δ (for example, their MLE's in the Z -module) are small so a prior ruling out large values with a big c_2 does not conflict the Z -data and c_2 can be very large (the upper bound on c_2 is there for numerical stability and doesn't reflect prior elicitation). When targeting Y , larger values of δ are needed, so c_1 is pulled up. This indicates conflict between the Y - and Z -modules. We learn from this analysis that the data are in conflict, and while there is too-little data to reliably inform c_1 and c_2 , the posterior and the ELPD are sensitive to the choice of c_1 and c_2 .

E.2.2 Supplementary figure for Section 6.2.2: SMI with the VMP and amortised prior hyperparameters

In this supplement section we give Figure 13 illustrating convergence of the optimisation of the ELPD over $\tilde{\psi}$ described in Section 6.2.2. We also give a comparison against MCMC of the fitted VMP targeting the SMI-posterior in (20) for the case of the generative model in (24). We show the marginal posteriors for selected δ -parameters in Figure 14.

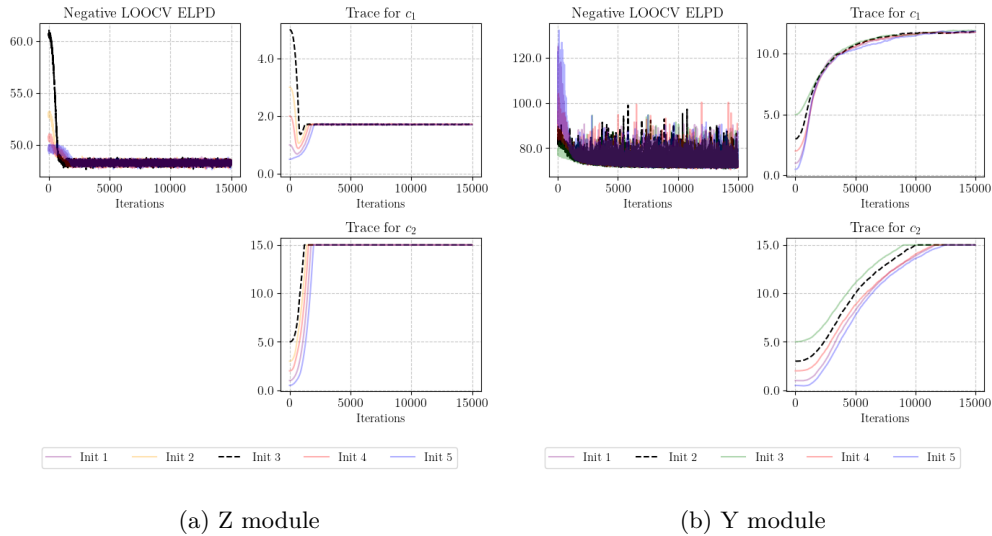


Figure 12: Epidemiological data in the Bayes setting of Section E.2.1 in this supplement. LOOCV loss and trace plots for hyperparameter optimisation at different initial values. The run achieving the lowest average loss over the last 20 iterations is the highlighted dashed line in black. Hyperparameters were selected as the average values over the 20 last iterations corresponding to the highlighted loss.

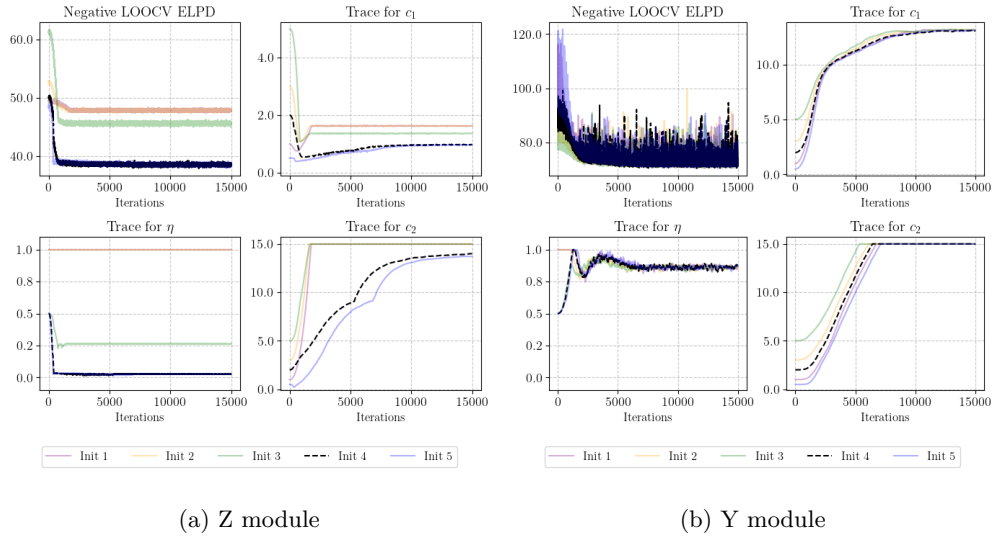


Figure 13: Epidemiological data in SMI setting of Section 6.2.2 in the main paper. LOOCV loss and trace plots for hyperparameter optimisation at different initial values. The run achieving the lowest average loss over the last 20 iterations is the highlighted dashed line in black. Hyperparameters were selected as the average values over the 20 last iterations corresponding to the highlighted loss.

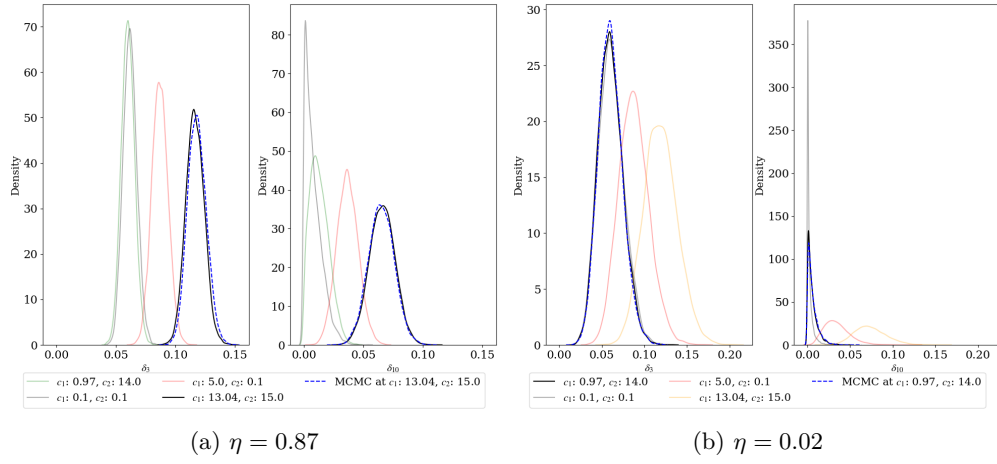


Figure 14: Epidemiological data in SMI setting. Solid lines: densities for VMP samples for δ_8 and δ_{10} at different prior hyperparameters; optimal prior hyperparameters in black. Blue dashed lines: MCMC samples at optimal prior hyperparameters.

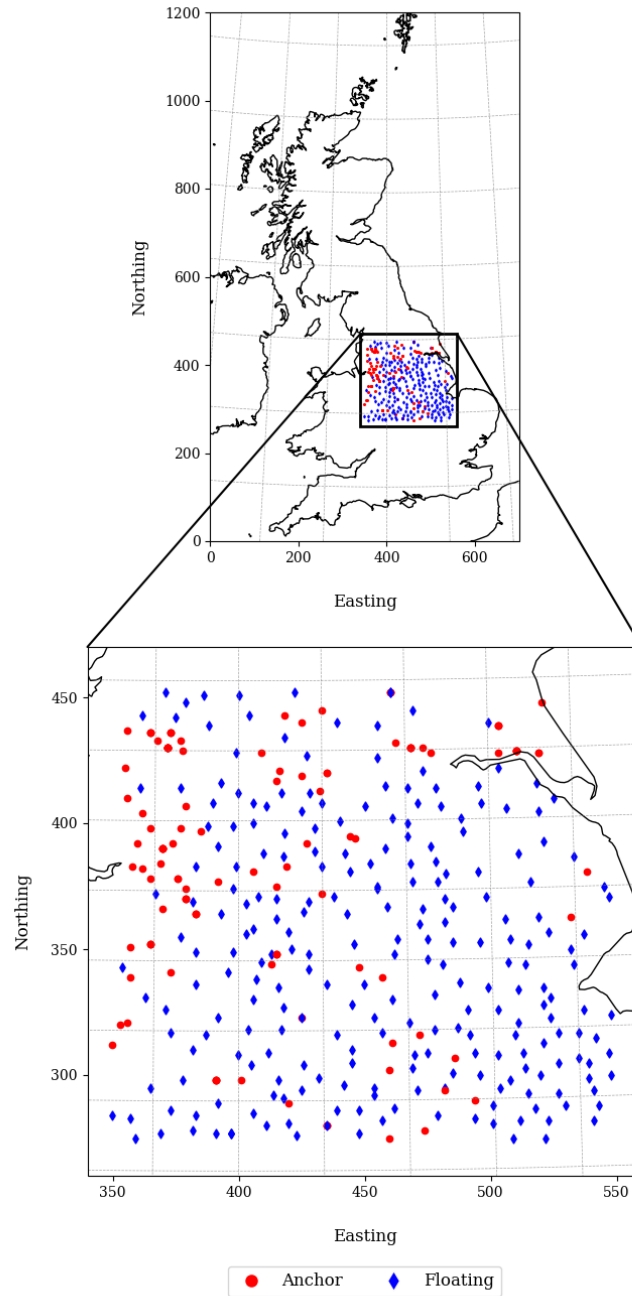


Figure 15: LALME data: a map outlining the exact location of the 120 anchor linguistic profiles and the Atlas estimates for the location of the 247 floating linguistic profiles. The focus is on a $200\text{km} \times 180\text{km}$ region in central Great Britain. The Atlas contains many profiles located outside the highlighted region.

E.3 LALME data

In this section we give additional information on the [Carmona et al. \(2024\)](#) study.

The data are 367 ‘‘Linguistic Profiles’’ (LPs) recording the presence and absence of 741 dialect spellings and grammatical forms across 367 documents from a 200km x 180km region in central Great Britain shown in Figure 15. These data are a subset of the Linguistic Atlas of Late Medieval English (LALME) ([McIntosh et al., 1986](#)), originally including 1044 LPs from text samples written in England, part of Wales and southern Scotland.

E.3.1 Additional background to the data and model

Data y_p at location x_p is assumed to be generated conditional on the local value $\Phi(x)$ of a multi-dimensional latent spatial field $\Phi : \mathcal{X} \rightarrow [0, 1]^{d_\phi}$, $d_\phi = \sum_{i=1}^I F_i$, and a set of other global parameters α . Each field component $\phi_{i,f}(x_p)$ represents the probability of an item i to take a particular form f , under the constraint that $\sum_{f=1}^{F_i} \phi_{i,f}(x_p) = 1 \forall i \in \mathcal{I}$ and $\forall p \in \mathcal{P}$.

The proposed observational model for the binary $y_{p,i,f}$ ’s takes $y_{p,i,f} = I(z_{p,i,f} > 0)$, where $z_{p,i,f}$ is the Poisson number of times word/item i in spelling/form f is used in LP p , with $z_{p,i,f} \sim \text{Poisson}(\mu_i \phi_{i,f}(x_p))$ assumed. Here μ_i represents the mean number of times item i is used across the corpus, while $\phi_{i,f}(x_p)$ is the probability that LP p uses item i in form f , under the constraint $\sum_{f=1}^{F_i} \phi_{i,f}(x_p) = 1$. Selection of form f is just a multinomial thinning of an overall Poisson count. Noting that

$$p(z_{p,i,f} = 0 | \mu_i, \phi_{i,f}(x_p)) = e^{-\mu_i \phi_{i,f}(x_p)} \quad (34)$$

and adding a parameter $\zeta_i \in [0, 1]$ to allow for an observed zero inflation, we obtain

$$p(Y_{\mathcal{P}} | \zeta, \mu, \Phi(X_{\mathcal{P}})) = \prod_{p \in \mathcal{P}} \prod_{i \in \mathcal{I}} \prod_{f=1}^{F_i} p(y_{p,i,f} | \zeta_i, \mu_i, \phi_{i,f}(x_p)) \quad (35)$$

$$= \prod_{p \in \mathcal{P}} \prod_{i \in \mathcal{I}} \prod_{f=1}^{F_i} \left[\zeta_i (1 - y_{p,i,f}) \right. \\ \left. + (1 - \zeta_i) (1 - e^{-\mu_i \phi_{i,f}(x_p)})^{y_{p,i,f}} (e^{-\mu_i \phi_{i,f}(x_p)})^{1 - y_{p,i,f}} \right] \quad (36)$$

The priors for item usage rates μ_i and zero inflation probability ζ_i are modelled as follows

$$p(\mu) = \prod_{i=1}^I p(\mu_i) = \prod_{i=1}^I \text{Gamma}(a, b) \quad (37)$$

$$p(\zeta) = \prod_{i=1}^I p(\zeta_i) = \prod_{i=1}^I \text{Uni}(0, 1) \quad (38)$$

The number of spatial fields $\phi_{i,f}(x_p)$ is large (741), and there is also anti-correlation across field values for item forms in each location (indicating a specific dialect prevalence), and positive correlation among item forms across locations (induced by a shared dialect). To reduce the dimensionality of the problem and induce correlation across items and forms at a given location, Carmona et al. (2024) parametrise the fields as a (soft-maxed) linear combination of a small number of shared basis fields $\gamma_b : \mathcal{X} \rightarrow \mathbb{R}$, $b \in \mathcal{B}$, $\mathcal{B} = \{1, \dots, B\}$, with B equal to 10, that only depend on location. To induce correlation across locations, the basis fields are modeled as Gaussian Processes (GPs) with a common exponential quadratic kernel $k(\cdot, \cdot)$ modeling spatial decay of correlation,

$$\begin{aligned}\phi_{i,f}(x_p) &= \frac{\exp(\gamma_{i,f}(x_p))}{\sum_{f' \in \mathcal{F}_i} \exp(\gamma_{i,f'}(x_p))} \\ \gamma_{i,f}(x_p) &= a_{i,f} + \sum_{b=1}^B \gamma_b(x_p) w_{i,f,b} \\ \gamma_b(x_p) &\sim GP(0, k(\cdot, \cdot)) \quad b \in \mathcal{B} = \{1, \dots, B\}\end{aligned}$$

Finally, the priors for the weights, off-sets and floating locations themselves are represented as

$$\begin{aligned}p(X_M) &= \prod_{p \in M} \text{Uni}(x_p \in \mathcal{X}) \\ p(a) &= \prod_{i=1}^I \prod_{f=2}^{F_i} p(a_{i,f}) = \prod_{i=1}^I \prod_{f=2}^{F_i} \text{Normal}(0, \sigma_a) \\ p(W) &= \prod_{b=1}^B \prod_{i=1}^I \prod_{f=1}^{F_i} p(w_{i,f,b}) = \prod_{b=1}^B \prod_{i=1}^I \prod_{f=1}^{F_i} \text{Laplace}(0, \sigma_w)\end{aligned}$$

Indicating all the *global* parameters with $\alpha = (\mu, \zeta, a, W)$, the joint distribution is

$$p(Y_{\mathcal{P}}, \alpha, \Gamma(X_{\mathcal{P}}), X_M) \equiv p(Y_{\mathcal{P}}, \alpha, \Gamma(X_{\mathcal{P}}), X_M) \quad (39)$$

$$= p(Y_A | \alpha, \Gamma(X_A)) \quad (40)$$

$$\times p(Y_M | \alpha, \Gamma(X_M)) \quad (41)$$

$$\times p(\Gamma(X_A), \Gamma(X_M) | X_M) \quad (42)$$

$$\times p(X_M) p(\alpha) \quad (43)$$

where for any set of profile labels $\mathcal{C} \subseteq \mathcal{P}$, $\Gamma(X_{\mathcal{C}}) = (\Gamma_b(X_{\mathcal{C}})_{b \in \mathcal{B}} = (\gamma_b(x_p))_{b \in \mathcal{B}}^{p \in \mathcal{C}}$.

For performing inference, the authors make use of approximations used in the GP-literature to circumvent the significant computational burdens coming with computing the joint distribution in Equation (43) exactly. This is because for each basis field b the joint distribution of $\Gamma_b(X_{\mathcal{P}})$ is a multivariate Gaussian with covariance matrix of

dimension $P \times P$, that will need to be inverted multiple times when targeting the posterior. Therefore, the authors target a sparse approximation of Equation (43) obtained via augmenting the prior with a set of $U = 121$ inducing points X_U , obtained by taking the vertices of a 10×10 homogeneous grid of the region of interest. Given the basis fields at the inducing points, $\Gamma(X_U)$, $\Gamma(X_A)$ are treated as independent of $\Gamma(X_M)$ (clearly an approximation), and thus the prior on basis fields becomes

$$p(\Gamma(X_A), \Gamma(X_M), \Gamma(X_U) | X_M) \approx p(\Gamma(X_A) | \Gamma(X_U)) p(\Gamma(X_M) | \Gamma(X_U), X_M) p(\Gamma(X_U)), \quad (44)$$

a product of multivariate Gaussians of lower dimension than P . Finally, the authors target a joint distribution integrated over $\Gamma(X_{\mathcal{P}})$ given $\Gamma(X_U)$ and X_M , namely

$$\begin{aligned} p(Y_{\mathcal{P}}, \alpha, \Gamma(X_U), X_M) &\simeq \mathbb{E}_{p(\Gamma(X_{\mathcal{P}} | \Gamma(X_U), X_M))} p(Y_{\mathcal{P}}, \alpha, \Gamma(X_{\mathcal{P}}), \Gamma(X_U), X_M) \\ &= \mathbb{E}_{p(\Gamma(X_A | \Gamma(X_U))} p(Y_A | \alpha, \Gamma(X_A), \Gamma(X_U)) \\ &\quad \times \mathbb{E}_{p(\Gamma(X_M | \Gamma(X_U), X_M))} p(Y_M | \alpha, \Gamma(X_M), \Gamma(X_U), X_M) \\ &\quad \times p(\Gamma(X_U), X_M, \alpha) \\ &= p(Y_A | \Gamma(X_U), \alpha) p(Y_M | \Gamma(X_U), \alpha, X_M) p(\Gamma(X_U), X_M, \alpha) \end{aligned} \quad (45)$$

The integration over $\Gamma(X_{\mathcal{P}})$ is common practice in variational work with Gaussian processes and is done to avoid fitting a joint distribution over field values $\Gamma(X_M)$ at random locations X_M .

In practice, we only ever need to evaluate the log-joint rather than the joint distribution and the expectations in (45) can be numerically unstable. Carmona et al. (2024) therefore make an additional approximation to compute the likelihoods for Y_A and Y_M , following Hensman et al. (2015), replacing them with the following lower bounds,

$$\log p(Y_A | \Gamma(X_U), \alpha) \geq E_{p(\Gamma(X_A) | \Gamma(X_U))} [\log p(Y_A | \alpha, \Gamma(X_A))] \quad (47)$$

$$\log p(Y_M | \Gamma(X_U), \alpha, X_M) \geq E_{p(\Gamma(X_M) | \Gamma(X_U), X_M)} [\log p(Y_M | \alpha, \Gamma(X_M))], \quad (48)$$

and these are estimated by averaging over joint samples $\Gamma(X_A) \sim p(\cdot | \Gamma(X_U))$ and $\Gamma(X_M) \sim p(\cdot | \Gamma(X_U), X_M)$. It follows that the joint distribution we target is

$$\begin{aligned} \log p(Y_{\mathcal{P}}, \alpha, \Gamma(X_U), X_M) &\simeq E_{p(\Gamma(X_M) | \Gamma(X_U), X_M)} [\log p(Y_M | \alpha, \Gamma(X_M))] \\ &\quad + E_{p(\Gamma(X_A) | \Gamma(X_U))} [\log p(Y_A | \alpha, \Gamma(X_A))] \\ &\quad + \log(p(\Gamma(X_U), X_M, \alpha)) \end{aligned} \quad (49)$$

Anticipating the results, the model is misspecified. This manifests itself as a ‘‘condensation’’ behavior: when the number of items $|Z|$ and floating profiles $|M|$ grows we cross a threshold where the posterior for the floating profiles concentrates onto the corners and boundaries of the region and the reconstructed float-locations X_M contradict the Atlas values. If $|Z|$ and $|M|$ are small, the posterior is well-behaved and the estimated float locations match Atlas values well. Model elaboration would be possible and may answer this issue. However, we can alternatively modify the inference and use SMI to carry out the analysis with all items and all floating profiles which is the approach taken here and in Carmona et al. (2024).

Parameter	Dimension	Full dataset	Small dataset
μ	I	71	5
ζ	I	71	5
a	$\sum f_i$	741	51
W	$B \sum f_i$	7,410	510
$\Gamma(X_U)$	BU	1,210	1,210
Subtotal (global params)		9,503	1,781
$X_{\bar{A}}$	$2M$	494	20
Subtotal (with floating locations)		9,997	1,801
$\Gamma(X_A)$	BN	1,200	1,200
$\Gamma(X_{\bar{A}})$	BM	2,470	100
Total		13,667	3,101

Table 2: LALME data: A summary of parameters and their dimensions.

E.3.2 Comparing the VMP to MCMC on a small dataset

In this section we show that the VMP gives good quality posterior approximation in this setting. MCMC on the (Bayes/ $\eta = 1$) posterior in (49) in Section E.3.1 of the Supplementary Material Battaglia and Nicholls (2024) is manageable for small data sets only, so although we retain all $|A| = 120$ anchor profiles we keep just $|M| = 10$ floating profiles and 5 randomly chosen items (“vpp”, “vps13”, “against”, “then”, “which”) coming in $d_\phi = 89$ forms. Retained profiles in M are selected so that their estimated locations cover \mathcal{X} evenly.

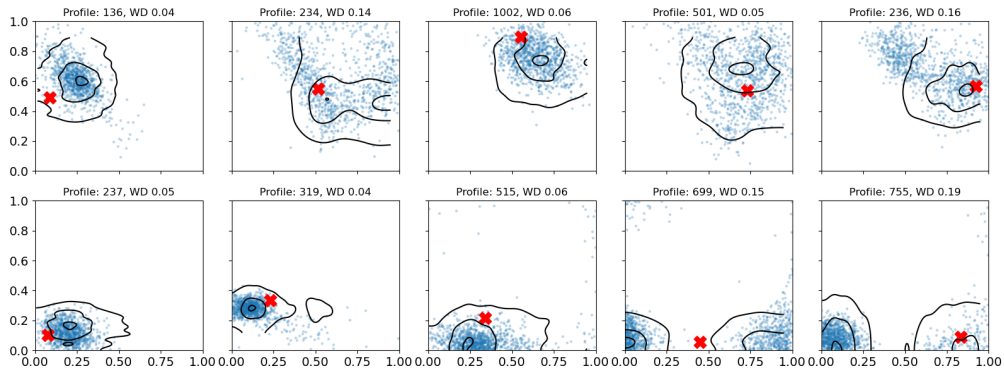
In this section we are demonstrating that the VMP accurately approximates Bayesian inference so we fix prior hyperparameters ψ in all analyses (see Section E.3.3 for detail), use MCMC to target (49) in Section E.3.1 and fit a VP to (49). We fit the VMP at all η -values (so $\tilde{\psi} = \{\eta\}$) and then evaluate the VMP at $\eta = 1$. We assign both VMP and VP the same hyperparameter tuning budget for the optimiser. The VMP should not be as accurate as the VP (the amortisation gap) so we wish to see how much we pay for amortising.

We consider the joint and marginal posterior distributions of the 10 floating profiles. Table 3 gives Wasserstein Distances between the MCMC baseline the variational approximations for these distributions. Both variational approximations show reasonable agreement to the MCMC output. Figure 16 gives a scatter-plot of MCMC samples, overlaid with the contours of the approximating VMP-posterior (top row) and those of the VP (bottom row). Carmona et al. (2024) gives the corresponding results for a VMP with the additive conditioner in (8). Performance is similar to our joint conditioner in (9) despite having 22500 less variational parameters. The VMP in (a) has comparable performance to a VP trained at $\eta = 1$ (b). For this small subset of the data, our estimated X_M are in fair agreement with Atlas-estimated locations (red crosses are

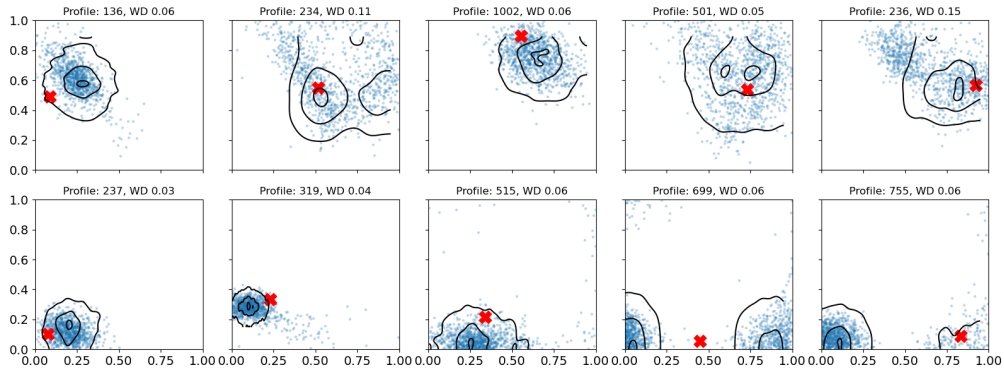
within contours, except profile 699, where the VMP is at least accurately fitting the true posterior).

	VMP	VP
Joint WD	0.45	0.30
WD	0.09(.02)	0.07(.01)

Table 3: Distance between MCMC distribution and VI approximation for the 10 floating profiles. First row: Wasserstein Distance between joint distributions of locations. Second row: mean of Wasserstein Distances (WD) between marginals for individual profile loctions; parentheses give standard deviation across profiles.



(a) VMP at $\eta = 1$



(b) VP for $\eta = 1$

Figure 16: LALME data in the Bayes setting, small data set of Section E.3.2. Scatter of MCMC samples for posterior locations of the 10 floating profiles, overlaid with the level sets of approximation with VMP (top row) and VP (bottom row). The red crosses give the Atlas estimates for the locations of these floating profiles.

E.3.3 Additional information on comparison to MCMC on the small dataset

The MCMC targets the standard Bayesian posterior as in Equation 47 after conditioning on $Y_{\mathcal{P}}$. For training, we use a standard No U-Turn Sampler (NUTS) (Hoffman et al., 2014) implemented in BlackJAX (Cabezas et al., 2024). Convergence was checked by visual inspection of MCMC traces for a large number of parameters.

For the variational models, we fix the prior hyperparameters to $\sigma_w = 5, \sigma_a = 10, a = 1, b = 0.5, \sigma_k = 0.2, \ell_k = 0.3$ as in Carmona et al. (2024). We use Hyper-Parameter Optimisation to select the decay factor and peak value for the AdaBelief learning rate schedule (Zhuang et al., 2020). The target metric to minimise was the minimum achieved joint Wasserstein Distance to the MCMC distribution over the 10 floating profiles. Search was performed via 40 Bayesian Optimisation (BP) jobs (Snoek et al., 2012) implemented with the Weights and Biases software (Biewald, 2020).

Figures 17 and 18 present additional plots on the performance of the the variational models with respect to MCMC on posterior inference for the ζ_i and μ_i .

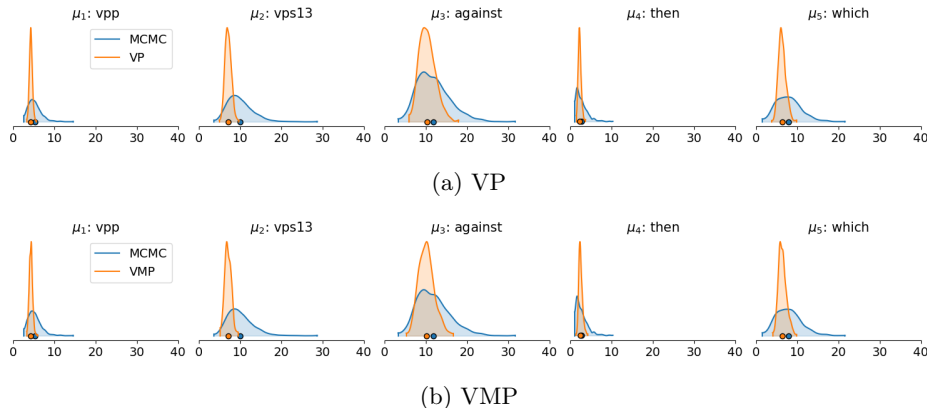
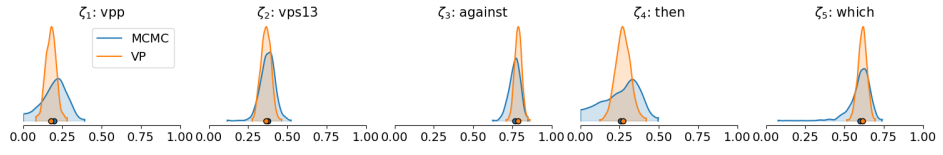
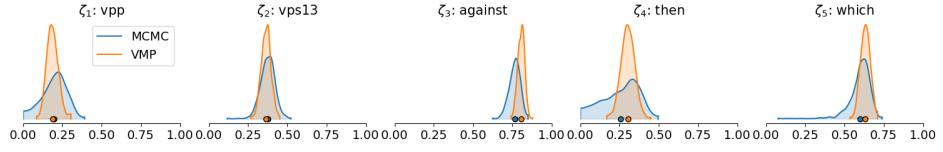


Figure 17: LALME small dataset. Comparison of MCMC to VI samples for μ on the small dataset across models.



(a) VP



(b) VMP

Figure 18: LALME small dataset. Comparison of MCMC to VI samples for ζ on the small dataset across VI models.

E.3.4 Additional information on inference on the full dataset

Figure 19 shows the VMP posterior approximations for ten randomly chosen floating LPs at optimal prior hyperparameters and varying η . Once again, we observe that a moderately sized η value improves inference by concentrating the distribution around the region approximately assigned by the fitting technique, without introducing excessive dispersion.

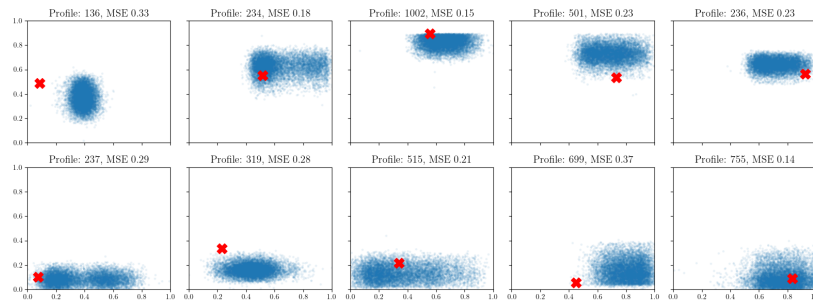
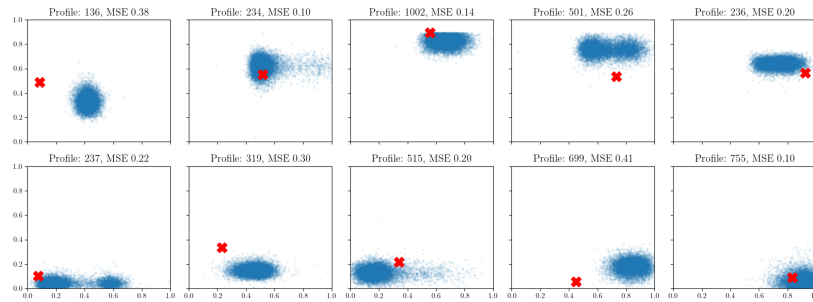
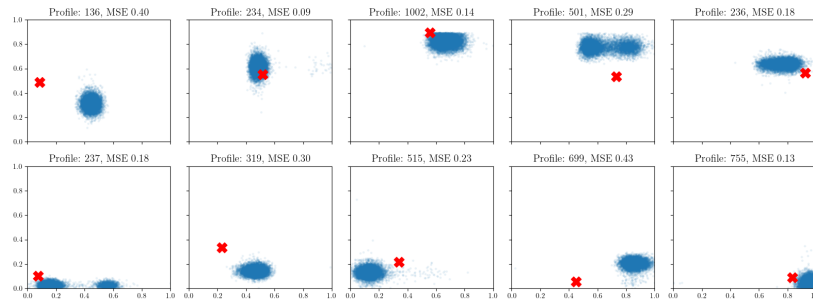
(a) $\eta = 0.0$ (b) $\eta = 0.42$ (c) $\eta = 1.0$

Figure 19: LALME data. VMP posterior approximations 10 floating LPs at optimal $\sigma_a = 5$, $\sigma_w = 10$, $\sigma_k = 0.4$, $\ell_k = 0.2$. Red crosses show fit-technique locations.

Figure 20 shows how the VP training loss (negative SMI-ELBO) of the fitted VP and VMP vary with η ; let $L_{VP}(\eta, \psi)$ and $L_{VMP}(\eta, \psi)$ denote these losses; we might expect $L_{VP}(\eta; \psi) < L_{VMP}(\eta; \psi)$ (an amortisation gap) as the “local” VP fits at fixed η, ψ while the VMP is one fit at all η, ψ . In this study prior hyperparameters $\sigma_a = 5$ and $\sigma_w = 10$ were kept fixed and we amortise the VMP over $\psi = (\sigma_k, \ell_k)$ and η . Once the VMP is trained, we fix an η -value and minimise the PMSE over ψ at that η to get ψ_η^* . This gives a point at $(\eta, L_{VMP}(\eta, \psi_\eta^*))$ on the VMP graph in Figure 20. The corresponding point $(\eta, L_{VP}(\eta, \psi_\eta^*))$ for the VP is obtained by fitting a VP at η, ψ_η^* so the VP is fitted six times and the VMP once. We see that the amortisation gap is negligible. In fact, the VMP achieves a slightly smaller loss than the VP for some η values, likely given a training advantage due to hyperparameter smoothing in the optimisation routine that compensates for the theoretical gap between the two models.

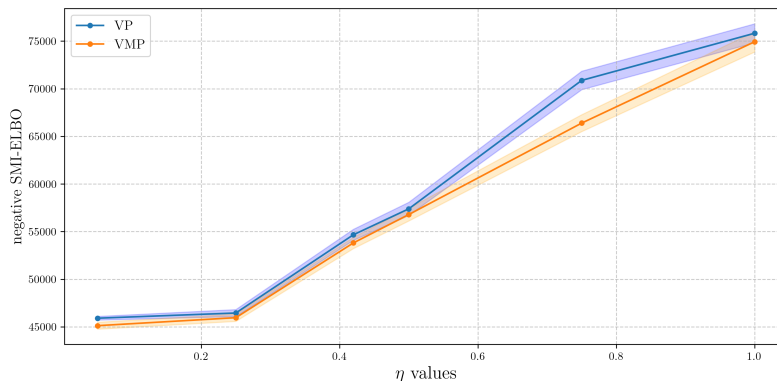


Figure 20: LALME data. Amortisation gap. Mean and $2\text{-}\sigma$ confidence interval for VMP and VP at different η values. The VMP line interpolates between the training loss values obtained by evaluating the negative SMI-ELBO at samples of a single trained VMP at different η . Negative SMI-ELBO values for the VP are obtained by refitting a different VP at each η value. At any given η , (σ_k, ℓ_k) set to the optimal values obtained by minimising the PMSE obtained from VMP samples at that η . $\sigma_a = 5$ and $\sigma_w = 10$ for any η .

Appendix F: Architecture, Hyperparameters and Runtime

The training of the VMP (and of the VP) utilises a variational family leveraging Neural Spline Flows as described in Durkan et al. (2019), stacking transforms with spline transformers and coupling conditioners. The VMP conditioners take as additional inputs ρ -samples for the hyperparameters of interest. We train the variational objective with an Adabelief optimiser (Zhuang et al., 2020) with a learning rate schedule. Table 4 presents the hyperparameters used for the algorithms in the different experiments. Table

5 reports the runtime and number of iterations for a single run of each algorithm, additionally comparing to MCMC where relevant. The VMP and VP have comparable runtimes per iteration. However, the VMP’s key advantage is that it requires only a single run to perform a comprehensive sensitivity analysis over the targeted inference hyperparameters. In contrast, the VP demands multiple runs to accomplish the same task, significantly increasing its overall computational cost.

The experiment infrastructure relies on modifications of the ModularBayes package for SMI (Carmona and Nicholls, 2022), and builds upon Distrax (DeepMind et al., 2020), a Python package implementing Normalising Flows in JAX (Bradbury et al., 2018). JAX is an open-source numerical computing library that extends NumPy functionality with automatic differentiation and GPU/TPU support, designed for high-performance machine learning research. All experiments were run on a Google Cloud Virtual Machine equipped with a v2 TPU with 8 cores, kindly provided by Google at no cost through the TPU Research Cloud (TRC) program.

Table 4: Hyperparameters for flow training.

Knots	Flow Layers	NN Width	NN Depth	LR peak value	LR decay rate	Experiment	Algorithm
10	4	5	3	3e-3	0.5	Synthetic	VMP
						Synthetic	VP
						Epidemiology Bayes	VMP
						Epidemiology SMI	VMP
10	8	30	5	0.13	6.4e-3	LP small	VMP
10	8	30	5	0.01	0.19	LP small	VP
10	6	30	5	3e-4	0.6	LP all	VMP
						LP all	VP

Table 5: Runtime and iterations for model training.

Experiment	Algorithm	Runtime	Iterations
Synthetic small	VMP	10m 26s	50,000
Synthetic small	VP	10m 48s	50,000
Synthetic small	MCMC	1m 3s	10,000
Synthetic large	VMP	16m 18s	50,000
Synthetic large	VP	16m 10s	50,000
Synthetic large	MCMC	29s	10,000
Epidemiology Bayes	VMP	13m 40s	50,000
Epidemiology Bayes	MCMC	2m 12s	10,000
Epidemiology SMI	VMP	14m 3s	50,000
Epidemiology SMI	MCMC	5m 8s	10,000
LP small	VMP	2h 5m 6s	200,000
LP small	VP	2h 14m 40s	200,000
LP small	MCMC	12h 21m 40s	50,000
LP all	VMP	2h 58m 40s	100,000
LP all	VP	2h 58m 49s	100,000

References

- Battaglia, L. and Nicholls, G. (2024). “Supplement of Amortising Variational Bayesian Inference over prior hyperparameters with a Normalising Flow.” DOI: 10.1214/[provided by typesetter]. 12, 19, 20
- Biewald, L. (2020). “Experiment Tracking with Weights and Biases.” Software available from wandb.com.
URL <https://www.wandb.com/> 22
- Bissiri, P. G., Holmes, C. C., and Walker, S. G. (2016). “A general framework for updating belief distributions.” *Journal of the Royal Statistical Society: Series B (Statistical Methodology)*, 78(5): 1103–1130.
URL <http://doi.wiley.com/10.1111/rssb.12158> 1, 10, 5
- Bradbury, J., Frostig, R., Hawkins, P., Johnson, M. J., Leary, C., Maclaurin, D., Necula, G., Paszke, A., VanderPlas, J., Wanderman-Milne, S., and Zhang, Q. (2018). “JAX: composable transformations of Python+NumPy programs.”
URL <http://github.com/google/jax> 26
- Cabezas, A., Corenflos, A., Lao, J., and Louf, R. (2024). “BlackJAX: Composable Bayesian inference in JAX.” 21, 22
- Carmona, C. U. and Nicholls, G. K. (2020). “Semi-Modular Inference: enhanced learning in multi-modular models by tempering the influence of components.” In Silvia, C. and Calandra, R. (eds.), *Proceedings of the 23rd International Conference on Artificial Intelligence and Statistics, AISTATS 2020*, 4226–4235. PMLR. ArXiv: 2003.06804.
URL <http://arxiv.org/abs/2003.06804> 3, 8, 9, 10, 14, 5
- (2022). “Scalable Semi-Modular Inference with Variational Meta-Posteriors.” ArXiv: 2204.00296.
URL <https://github.com/chriscarmona/modularbayes> 1, 2, 3, 4, 7, 9, 10, 11, 5, 6, 26
- Chakraborty, A., Nott, D. J., Drovandi, C., Frazier, D. T., and Sisson, S. A. (2022). “Modularized Bayesian analyses and cutting feedback in likelihood-free inference.” ArXiv: 2203.09782.
URL <http://arxiv.org/abs/2203.09782> 5
- Chen, X., Kingma, D. P., Salimans, T., Duan, Y., Dhariwal, P., Schulman, J., Sutskever, I., and Abbeel, P. (2016). “Variational lossy autoencoder.” *arXiv preprint arXiv:1611.02731*. 1
- DeepMind, Babuschkin, I., Baumli, K., Bell, A., Bhupatiraju, S., Bruce, J., Buchlovsky, P., Budden, D., Cai, T., Clark, A., Danihelka, I., Dedieu, A., Fantacci, C., Godwin, J., Jones, C., Hemsley, R., Hennigan, T., Hessel, M., Hou, S., Kapturowski, S., Keck, T., Kemaev, I., King, M., Kunesch, M., Martens, L., Merzic, H., Mikulik, V., Norman, T., Papamakarios, G., Quan, J., Ring, R., Ruiz, F., Sanchez, A., Sartran, L., Schneider, R., Sezener, E., Spencer, S., Srinivasan, S., Stanojević, M., Stokowiec, W., Wang, L., Zhou, G., and Viola, F. (2020). “The DeepMind JAX Ecosystem.”
URL <http://github.com/deepmind> 26

- Dinh, L., Sohl-Dickstein, J., and Bengio, S. (2016). “Density estimation using Real NVP.” In *Proceedings of the 5th International Conference on Learning Representations, ICLR 2017*. ArXiv: 1605.08803.
URL <http://arxiv.org/abs/1605.08803> 2, 1
- Durkan, C., Bekasov, A., Murray, I., and Papamakarios, G. (2019). “Neural Spline Flows.” In *Proceedings of the 33rd Conference on Neural Information Processing Systems, NeurIPS 2019*. ArXiv: 1906.04032.
URL <http://arxiv.org/abs/1906.04032> 2, 5, 1, 25
- Frazier, D. T. and Nott, D. J. (2023a). “Accurate semi-modular posterior inference with a user-defined loss function.”
URL <https://arxiv.org/abs/2301.10911> 2, 11, 5
- (2023b). “Cutting feedback and modularized analyses in generalized Bayesian inference.”
URL <https://arxiv.org/abs/2202.09968> 11, 5
- Hensman, J., Matthews, A., and Ghahramani, Z. (2015). “Scalable variational Gaussian process classification.” In *Artificial Intelligence and Statistics*, 351–360. PMLR. 19
- Hoffman, M. D., Gelman, A., et al. (2014). “The No-U-Turn sampler: adaptively setting path lengths in Hamiltonian Monte Carlo.” *J. Mach. Learn. Res.*, 15(1): 1593–1623. 21, 22
- Huang, C.-W., Krueger, D., Lacoste, A., and Courville, A. (2018). “Neural Autoregressive Flows.” In Dy, J. and Krause, A. (eds.), *Proceedings of the 35th International Conference on Machine Learning*, volume 80 of *Proceedings of Machine Learning Research*, 2078–2087. PMLR.
URL <https://proceedings.mlr.press/v80/huang18d.html> 2, 5, 6, 7, 1, 3
- Jacob, P. E., Murray, L. M., Holmes, C. C., and Robert, C. P. (2017). “Better together? Statistical learning in models made of modules.” ArXiv: 1708.08719 Pages: 1-31.
URL <http://arxiv.org/abs/1708.08719> 5
- Jacob, P. E., O’Leary, J., and Atchadé, Y. F. (2020). “Unbiased Markov Chain Monte Carlo Methods with Couplings.” *Journal of the Royal Statistical Society Series B: Statistical Methodology*, 82(3): 543–600.
URL <https://doi.org/10.1111/rssb.12336> 5
- Jaini, P., Selby, K. A., and Yu, Y. (2019). “Sum-of-squares polynomial flow.” In *International Conference on Machine Learning*, 3009–3018. PMLR. 5, 1
- Kingma, D. P. and Dhariwal, P. (2018). “Glow: Generative flow with invertible 1x1 convolutions.” *Advances in neural information processing systems*, 31. 1
- Kingma, D. P., Salimans, T., Jozefowicz, R., Chen, X., Sutskever, I., and Welling, M. (2016). “Improved variational inference with inverse autoregressive flow.” *Advances in neural information processing systems*, 29. 1
- Liu, F., Bayarri, M. J., and Berger, J. O. (2009). “Modularization in Bayesian analysis, with emphasis on analysis of computer models.” *Bayesian Analysis*, 4(1): 119–150.

ISBN: 1936-0975.

URL <http://projecteuclid.org/euclid.ba/1340370392> 5

Liu, Y. and Goudie, R. J. B. (2022a). “A General Framework for Cutting Feedback within Modularized Bayesian Inference.” ArXiv:2211.03274 [math, stat].

URL <http://arxiv.org/abs/2211.03274> 5

— (2022b). “Stochastic approximation cut algorithm for inference in modularized Bayesian models.” *Statistics and Computing*, 32(1): 7. ArXiv: 2006.01584.

URL <http://arxiv.org/abs/2006.01584> 5

Lunn, D., Best, N., Spiegelhalter, D., Graham, G., and Neuenschwander, B. (2009). “Combining MCMC with ‘sequential’PKPD modelling.” *Journal of Pharmacokinetics and Pharmacodynamics*, 36: 19–38. 11, 5

McIntosh, A., Samuels, M. L., Benskin, M., Laing, M., and Williamson, K. (1986). *A linguistic atlas of late mediaeval English*. Aberdeen University Press. 15, 17

Meng, X.-L. (1994). “Multiple-Imputation Inferences with Uncongenial Sources of Input.” *Statistical Science*, 9(4): 538 – 558.

URL <https://doi.org/10.1214/ss/1177010269> 11, 5

Morrow, R. and Chiu, W.-C. (2020). “Variational autoencoders with normalizing flow decoders.” *arXiv preprint arXiv:2004.05617*. 1

Nicholls, G. K., Lee, J. E., Wu, C.-H., and Carmona, C. U. (2022). “Valid belief updates for prequentially additive loss functions arising in Semi-Modular Inference.” ArXiv:2201.09706 [stat].

URL <http://arxiv.org/abs/2201.09706> 5

Papamakarios, G., Nalisnick, E., Rezende, D. J., Mohamed, S., and Lakshminarayanan, B. (2021). “Normalizing Flows for Probabilistic Modeling and Inference.” *J. Mach. Learn. Res.*, 22(1). 2, 5, 6, 7, 1, 3

Papamakarios, G., Pavlakou, T., and Murray, I. (2017). “Masked autoregressive flow for density estimation.” *Advances in neural information processing systems*, 30. 1

Plummer, M. (2015). “Cuts in Bayesian graphical models.” *Statistics and Computing*, 25(1): 37–43.

URL <http://link.springer.com/10.1007/s11222-014-9503-z> 11, 13, 5

Pompe, E. and Jacob, P. E. (2021). “Asymptotics of cut distributions and robust modular inference using Posterior Bootstrap.” *arXiv preprint arXiv:2110.11149*. 5

Rezende, D. and Mohamed, S. (2015). “Variational inference with normalizing flows.” In *International conference on machine learning*, 1530–1538. PMLR. 2, 8, 1

Snoek, J., Larochelle, H., and Adams, R. P. (2012). “Practical Bayesian Optimization of Machine Learning Algorithms.” In *Advances in Neural Information Processing Systems*, volume 25. Curran Associates, Inc.

URL <https://papers.nips.cc/paper/2012/hash/05311655a15b75fab86956663e1819cd-Abstract.html> 22

- Tabak, E. G. and Turner, C. V. (2013). “A family of nonparametric density estimation algorithms.” *Communications on Pure and Applied Mathematics*, 66(2): 145–164. 1
- Tabak, E. G. and Vanden-Eijnden, E. (2010). “Density estimation by dual ascent of the log-likelihood.” *Communications in Mathematical Sciences*, 8(1): 217–233. 1
- Yu, X., Nott, D. J., and Smith, M. S. (2023). “Variational inference for cutting feedback in misspecified models.” *Statistical Science*, 38(3): 490–509. 5
- Zhang, Y., Sadeghi, A., and Giannakis, G. B. (2024). “Meta-Learning Universal Priors Using Non-Injective Normalizing Flows.”
URL <https://openreview.net/forum?id=sKqGVqkvuS> 1
- Zhuang, J., Tang, T., Ding, Y., Tatikonda, S., Dvornek, N., Papademetris, X., and Duncan, J. S. (2020). “AdaBelief Optimizer: Adapting Stepsizes by the Belief in Observed Gradients.” ArXiv:2010.07468 [cs, stat].
URL <http://arxiv.org/abs/2010.07468> 22, 25